Available online at www.sciencedirect.com

SciVerse ScienceDirect

Nuclear Physics B 870 (2013) 323–352

NUCLEAR PHYSICS B

www.elsevier.com/locate/nuclphysb

Natural NMSSM Higgs bosons

S.F. King [a], M. Mühlleitner [b,*], R. Nevzorov [c], K. Walz [b]

[a] *School of Physics and Astronomy, University of Southampton, Southampton, SO17 1BJ, UK*
[b] *Institute for Theoretical Physics, Karlsruhe Institute of Technology, 76128 Karlsruhe, Germany*
[c] *Institute for Theoretical and Experimental Physics, Moscow 117218, Russia*

Received 28 November 2012; accepted 21 January 2013

Available online 1 February 2013

Abstract

We study the phenomenology of Higgs bosons close to 126 GeV within the scale invariant unconstrained Next-to-Minimal Supersymmetric Standard Model (NMSSM), focusing on the regions of parameter space favoured by low fine-tuning considerations, namely stop masses of order 400 GeV to 1 TeV and an effective μ parameter between 100–200 GeV, with large (but perturbative) λ and low $\tan\beta = 2$–4. We perform scans over the above parameter space, focusing on the observable Higgs cross sections into $\gamma\gamma$, WW, ZZ, bb, $\tau\tau$ final states, and study the correlations between these observables. We show that the $\gamma\gamma$ signal strength may be enhanced up to a factor of about two not only due to the effect of singlet–doublet mixing, which occurs more often when the 126 GeV Higgs boson is the next-to-lightest CP-even one, but also due to light stops (and to a lesser extent light chargino and charged Higgs loops). There may be also smaller enhancements in the Higgs decay channels into WW, ZZ, correlated with the $\gamma\gamma$ enhancement. However there is no such correlation observed involving the Higgs decay channels into bb, $\tau\tau$. The requirement of having perturbative couplings up to the GUT scale favours the interpretation of the 126 GeV Higgs boson as being the second lightest NMSSM CP-even state, which can decay into pairs of lighter neutralinos, CP-even or CP-odd Higgs bosons, leading to characteristic signatures of the NMSSM. In a non-negligible part of the parameter range the increase in the $\gamma\gamma$ rate is due to the superposition of rates from nearly degenerate Higgs bosons. Resolving these Higgs bosons would rule out the Standard Model, and provide evidence for the NMSSM.

* Corresponding author.
E-mail addresses: king@soton.ac.uk (S.F. King), maggie@particle.uni-karlsruhe.de (M. Mühlleitner), nevzorov@itep.ru (R. Nevzorov), kwalz@particle.uni-karlsruhe.de (K. Walz).

0550-3213
http://dx.doi.org/10.1016/j.nuclphysb.2013.01.020

1. Introduction

The recent discovery of a new particle with a mass around ∼125 GeV [1,2] is consistent with the Standard Model (SM) Higgs boson. In particular the observed decays and signal strengths into $\gamma\gamma$, WW, ZZ favour the interpretation that the particle is a neutral boson with spin-0. However more data is needed to assess its nature, and if careful studies of the signal strengths in different channels reveal discrepancies from the predictions of the SM then this would provide a window into new physics Beyond the Standard Model (BSM) [3]. Supersymmetric (SUSY) models are a leading candidate for BSM physics and generically predict one or more light Higgs bosons whose properties may differ in detail from that of the SM Higgs boson. For example, if the cross section of Higgs production and decay into $\gamma\gamma$ were observed to be significantly higher than the SM Higgs prediction, then this could be due to the effects of SUSY particles in the loops [4–13] or suppressed couplings to b quarks leading to smaller total widths [9–24].

In the Minimal Supersymmetric Standard Model (MSSM) there exists an upper limit on the lightest Higgs boson mass of about 130–135 GeV, depending on the values of the parameters in the stop sector (see *e.g.* [25] and references therein). The MSSM can be consistent with a 126 GeV SM-like Higgs boson in the decoupling limit. In this limit the lightest Higgs boson mass is given by

$$m_h^2 \approx M_Z^2 \cos^2 2\beta + \Delta m_h^2, \tag{1.1}$$

with the correction Δm_h^2 being dominated by loops of heavy top quarks and top squarks. The ratio of the Vacuum Expectation Values (VEVs) of the two Higgs doublets introduced in the MSSM Higgs sector is denoted by $\tan\beta$. In order to raise the Higgs boson mass to 126 GeV, we hence need at large values of $\tan\beta$ a loop contribution of $\Delta m_h \approx 85$ GeV which is nearly as large as the tree-level mass value. This leads to some degree of fine-tuning [26].

It has been known for some time that the fine-tuning of the MSSM could be ameliorated in the scale invariant Next-to-Minimal Supersymmetric Standard Model (NMSSM) [27,28]. With a 126 GeV Higgs boson, due to the fine-tuning of the MSSM, the NMSSM has emerged as a more natural alternative. In the NMSSM [29–32] (for reviews see [33,34]) one singlet superfield S is added to the spectrum of the MSSM. The supersymmetric Higgs mass parameter μ is then generated dynamically through the coupling term $\lambda S H_d H_u$. The upper mass bound of the lightest Higgs boson in the NMSSM becomes

$$m_h^2 \approx M_Z^2 \cos^2 2\beta + \frac{\lambda^2 v^2}{2} \sin^2 2\beta + \Delta m_h^2, \tag{1.2}$$

where $v = 246$ GeV. Contrary to the MSSM, for $\lambda v > M_Z$, the tree-level contributions to m_h are maximised for moderate values of $\tan\beta$. For example, setting $\lambda = 0.6$ and $\tan\beta = 2$, these tree-level contributions raise the Higgs boson mass to about 100 GeV requiring $\Delta m_h \sim 75$ GeV in order to match the 126 GeV Higgs mass value. The difference to the correction needed in the MSSM (numerically about 10 GeV) is significant as Δm_h raises logarithmically with the stop masses and receives an important contribution from the stop mixing.

In the NMSSM, depending on $\tan\beta$, $\lambda \sim 0.7$ is the largest value in order not to spoil the validity of perturbation theory up to the GUT scale. The presence of additional extra matter, however, allows larger values of λ to be achieved [35]. For example, adding three families of $5 + \bar{5}$ extra matter at a mass scale of 1 TeV increases the largest value to $\lambda \sim 0.8$ for the same parameters as before. The above discussion shows that there is an argument from fine-tuning for extending the NMSSM to include extra matter. Such an NMSSM+ model with extra matter has recently been discussed in [36].

In this paper we study the phenomenology of Higgs bosons in the mass range 124–127 GeV within the scale invariant NMSSM. To distinguish our study from the many NMSSM studies in the literature of a near 126 GeV Higgs boson, we shall focus exclusively on the regions of parameter space favoured by low fine-tuning considerations, namely stop masses of order 400 GeV to 1 TeV and an effective μ parameter between 100–200 GeV, with large (but perturbative) λ and low $\tan\beta = 2$–4. We shall allow for the possibility of extending the NMSSM to include extra matter as in the NMSSM+ [36], so that λ can be increased up to 0.8 at low-energy scales, while remaining perturbative up to the GUT scale. We perform scans over the above parameter space, focusing on the observable Higgs cross sections into $\gamma\gamma$, WW, ZZ, bb, $\tau\tau$ final states, and study the correlations between these observables. We show that the $\gamma\gamma$ signal strength may be enhanced up to a factor of two due to an enhancement of the production and/or the decay mechanism. While small stop mixing for light stops enhances the dominant production process through gluon fusion and suppresses the loop-mediated decay into photons, the latter can also be enhanced to some extent through light chargino and charged Higgs boson loops. Furthermore, the suppression of the dominant decay into bottom quarks due to singlet–doublet mixing entails a suppressed total width and hence enhances the branching ratio into photons. Since also the branching ratios into WW and ZZ are affected by such a suppression there is a strong correlation between these channels and the $\gamma\gamma$ enhancement. However there is no such correlation observed involving the Higgs decay channels into bb, $\tau\tau$ which may be suppressed in the enhanced $\gamma\gamma$ region. The results include the possible presence of a second Higgs boson in the region of 126 GeV. The superposition of the rates of two nearly degenerate Higgs bosons also increases the event rate in the photon final state. Provided that such a signal can be disentangled from a singly produced Higgs boson in future, this will be a further strong test of the NMSSM. Our scan reveals that with the chosen small stop mass values it is difficult to get a lightest CP-even Higgs boson with mass around 126 GeV if in addition perturbativity constraints are imposed. It can only be achieved for large mixing values and inclusion of extra matter at $\sim$1 TeV, while this is not necessary if the second lightest CP-even Higgs boson is demanded to have the same mass as the recently discovered new resonance. Interestingly, in this case the mass spectrum can be such that the heavier CP-even Higgs boson can decay into a pair of lightest neutralinos, CP-odd or CP-even Higgs bosons, which leads to distinctive final state signatures to be tested at the LHC.

The work in this paper complements and goes beyond the other studies of a Higgs boson near 126 GeV in the NMSSM [11–15,19,21–24,28,37–44]. For example the original observation that the di-photon channel may be enhanced due to strong singlet–doublet mixing due to the reduction of the bb partial width with a second lighter CP-even Higgs boson was made in [14]. This was followed by our proposal [19] of a set of benchmark points in which we studied, in addition to $\gamma\gamma$ and bb, also the channels WW and ZZ both for the case where the second CP-even Higgs boson is lighter or heavier than the 126 GeV one, for the case of light top squarks and gluinos. The channels were also studied in the framework of various versions of the constrained NMSSM with relatively heavy stops [37], and a comparative study between the MSSM and NMSSM has been performed in [21]. In [22] the effect of astrophysical and Dark Matter (DM) constraints on the Lightest Supersymmetric Particle (LSP) in the NMSSM with a 126 GeV Higgs boson was taken into account with the main focus on the LSP being a singlino-like neutralino. Similar constraints were also applied to the constrained NMSSM with a dominantly Higgsino-like LSP [23]. The case of the Higgs boson mass spectrum in the complex NMSSM was considered in [38] leading to significant effects on Higgs phenomenology. In [39] scenarios were investigated where the two lightest NMSSM Higgs bosons are closely spaced near 126 GeV, leading to very enhanced decay rates, and in [24] scenarios with Higgs bosons both consistent with the

LEP 98 GeV excess and the 126 GeV Higgs boson of the LHC search were studied, while [12] discussed the case where the NMSSM Higgs sector could both explain the 126 GeV discovery and the small excess observed by CMS at 136 GeV. In [40] a more complicated non-NMSSM model with extra singlets was proposed, while in [41] another alternative to the NMSSM involving singlet mass terms was studied. The case of fine-tuning in the NMSSM was analysed in [27]. Finally, the effects of combining the NMSSM with an inverse see-saw mechanism were considered in [42].

The layout of the remainder of this paper is as follows. In Section 2 we briefly introduce the Higgs sector of the scale invariant NMSSM. In Section 3 we present in detail the parameter values which we choose for the scan in the NMSSM parameter space. This is followed, in Section 4, by the discussion of the SUSY particle effects in the loop-mediated processes of the dominant NMSSM Higgs production through gluon fusion on the one hand and the decay into a photon pair on the other hand. Section 5 contains the numerical analysis with the presentation and discussion of λ–κ and mass distributions, of total widths, branching ratios and reduced rates with their correlations. A comparison with the present LHC Higgs search results is presented. Section 6 summarises and concludes the paper.

2. The NMSSM

We restrict ourselves to the NMSSM with a scale invariant superpotential. We do not take into account other possible extensions as the Minimal–Non-minimal Supersymmetric SM (MNSSM), new minimally-extended supersymmetric SM or nearly-Minimal Supersymmetric SM (nMSSM), neither extensions with additional $U(1)'$ gauge symmetries [45], nor the case of explicit CP violation [38,46,47].

Including only the third generation fermions, the NMSSM superpotential in terms of (hatted) superfields is given by

$$\mathcal{W} = \lambda \hat{S} \hat{H}_u \hat{H}_d + \frac{\kappa}{3} \hat{S}^3 + h_t \hat{Q}_3 \hat{H}_u \hat{t}^c_R - h_b \hat{Q}_3 \hat{H}_d \hat{b}^c_R - h_\tau \hat{L}_3 \hat{H}_d \hat{\tau}^c_R. \tag{2.3}$$

The first term replaces the μ-term $\mu \hat{H}_u \hat{H}_d$ of the MSSM superpotential, while the second one, cubic in the singlet superfield, is introduced to break the Peccei–Quinn symmetry [48] in order to avoid the appearance of a massless axion. The last three terms represent the Yukawa interactions. The scalar mass parameters for the Higgs and sfermion scalar fields which contribute to the soft SUSY breaking Lagrangian read in terms of the fields corresponding to the complex scalar components of the superfields,

$$\begin{aligned} -\mathcal{L}_{\text{mass}} = {} & m^2_{H_u} |H_u|^2 + m^2_{H_d} |H_d|^2 + m^2_S |S|^2 \\ & + m^2_{\tilde{Q}_3} \left|\tilde{Q}^2_3\right| + m^2_{\tilde{t}_R} \left|\tilde{t}^2_R\right| + m^2_{\tilde{b}_R} \left|\tilde{b}^2_R\right| + m^2_{\tilde{L}_3} \left|\tilde{L}^2_3\right| + m^2_{\tilde{\tau}_R} \left|\tilde{\tau}^2_R\right|. \end{aligned} \tag{2.4}$$

And the trilinear soft SUSY breaking interactions between the sfermion and Higgs fields are

$$\begin{aligned} -\mathcal{L}_{\text{tril}} = {} & \lambda A_\lambda H_u H_d S + \frac{1}{3} \kappa A_\kappa S^3 + h_t A_t \tilde{Q}_3 H_u \tilde{t}^c_R - h_b A_b \tilde{Q}_3 H_d \tilde{b}^c_R \\ & - h_\tau A_\tau \tilde{L}_3 H_d \tilde{\tau}^c_R + \text{h.c.} \end{aligned} \tag{2.5}$$

We work in the unconstrained NMSSM with non-universal soft terms at the GUT scale. The three SUSY breaking masses squared for H_u, H_d and S which appear in $\mathcal{L}_{\text{mass}}$ can be expressed through their VEVs by exploiting the three minimisation conditions of the scalar potential. While

the MSSM Higgs sector at tree-level can be described by only two free parameters (in general chosen to be the mass of the pseudoscalar Higgs boson and $\tan\beta$), the Higgs sector of the NMSSM is parameterised by the six parameters

$$\lambda, \quad \kappa, \quad A_\lambda, \quad A_\kappa, \quad \tan\beta = \langle H_u\rangle/\langle H_d\rangle \quad \text{and} \quad \mu_{\text{eff}} = \lambda\langle S\rangle. \tag{2.6}$$

The brackets denote the VEV of the respective field inside. The sign conventions are chosen such that λ and $\tan\beta$ are positive, whereas κ, A_λ, A_κ and μ_{eff} can have both signs.

The Higgs sector consists of 3 CP-even Higgs bosons H_i ($i = 1, 2, 3$), two CP-odd states A_j ($j = 1, 2$) and two charged Higgs scalars $H^\pm$. The neutral Higgs bosons are ordered by ascending mass with H_1 (A_1) being the lightest CP-even (odd) Higgs boson. As higher order corrections to the Higgs sector are important and have to be considered in order to calculate the Higgs sector as accurately as possible, also the parameters from the non-Higgs sector, which enter through the loop corrections, have to be specified. These are the soft SUSY breaking mass terms in Eq. (2.4) for the scalars as well as the trilinear couplings in Eq. (2.5) and the gaugino soft SUSY breaking mass parameters given by

$$-\mathcal{L}_{\text{gauginos}} = \frac{1}{2}\left[M_1 \tilde{B}\tilde{B} + M_2 \sum_{a=1}^{3} \tilde{W}^a \tilde{W}_a + M_3 \sum_{a=1}^{8} \tilde{G}^a \tilde{G}_a + \text{h.c.} \right]. \tag{2.7}$$

3. The scan

In the following we will perform a scan in the NMSSM parameter space in order to investigate the Higgs sector in view of the recent LHC Higgs search results together with the resulting possible theoretical and phenomenological implications. When performing our scan we seek to generate a Higgs spectrum where one of the scalar Higgs bosons corresponds to a state with mass value around 126 GeV leading to event rates in its production which are compatible with the LHC results. We furthermore keep the fine-tuning [18,19,26,27] as low as possible by demanding light top squark masses and/or small mixing in the stop sector.

For the calculation of the SUSY particle and NMSSM Higgs boson spectrum and branching ratios we use the program package `NMSSMTools` [49,50]. The higher order corrections to the NMSSM Higgs boson masses are important [51] and have been included in `NMSSMTools` up to $\mathcal{O}(\alpha_t\alpha_s + \alpha_b\alpha_s)$ for vanishing external momentum. Within the package the Fortran code `NMHDECAY` [49], an NMSSM extension of the Fortran code `HDECAY` [52,53], provides the Higgs decay widths and branching ratios, while the SUSY particle branching ratios are obtained from the Fortran code `NMSDECAY` [54] based on the generalisation of the Fortran code `SDECAY` [53, 55] to the NMSSM particle spectrum. The output of the NMSSM particle spectrum, mixing angles, decay widths and branching ratios is provided in the SUSY Les Houches Accord (SLHA) format [56]. Being interfaced with `micrOMEGAs` [57], also the relic abundance of the lightest neutralino $\tilde{\chi}_1^0$ as the NMSSM Dark Matter candidate can be evaluated with `NMSSMTools`. Furthermore, the package checks for the constraints from low-energy observables as well as from Tevatron and LEP. For details, we refer the reader to the program webpage [50].[1]

In order to restrict the parameter range for our scan we are guidelined by the following objectives which follow from theoretical and experimental considerations:

[1] Concerning the value of $g-2$, it is non-trivial to find parameter combinations which can explain the 2σ deviation from the SM value. In our analysis we do not further consider this constraint.

- To keep the Higgs mass corrections (governed by the corrections from the (s)top sector) and hence the amount of fine-tuning as low as possible, the tree-level mass of the lightest Higgs boson is maximised by fixing $\tan\beta$ to small values chosen as

$$\tan\beta = 2, 4. \tag{3.8}$$

- Also the effective $\mu_{\rm eff}$ parameter is kept as low as possible in order to avoid fine-tuning. It is varied in the range

$$100\ \text{GeV} \leqslant \mu_{\rm eff} \leqslant 200\ \text{GeV}. \tag{3.9}$$

  Although we did not further consider the constraint coming from the anomalous magnetic moment of the muon, we decided to take positive values of $\mu_{\rm eff}$ as, similarly to the MSSM μ parameter, positive values are favoured when this constraint is included, see *e.g.* [11].
- We shall be interested exclusively in large values of λ in order to increase the tree-level mass of the CP-even Higgs boson associated with the 126 GeV Higgs boson resonance. At the same time we pay attention that it remains small enough to ensure the validity of perturbation theory up to large scales, chosen to be the GUT scale here. This also constrains possible values of κ. Based on the results from the two-loop renormalisation group running down to 1 TeV with and without the possibility of exotic extra matter [19] we hence perform our scan in the ranges

$$0.55 \leqslant \lambda \leqslant 0.8 \quad \text{and} \quad 10^{-4} \leqslant \kappa \leqslant 0.4. \tag{3.10}$$

- The soft SUSY breaking trilinear couplings A_λ and A_κ are varied in the ranges

$$-500\ \text{GeV} \leqslant A_\kappa \leqslant 0\ \text{GeV} \quad \text{and} \quad 200\ \text{GeV} \leqslant A_\lambda \leqslant 800\ \text{GeV}. \tag{3.11}$$

- For fine-tuning reasons we keep the soft SUSY breaking masses of the stop sector rather low and vary them simultaneously as

$$500\ \text{GeV} \leqslant M_{\tilde{Q}_3} = M_{\tilde{t}_R} \leqslant 800\ \text{GeV}. \tag{3.12}$$

  For A_U $(U \equiv u, c, t)$[2] we choose two representative values corresponding to low and large mixings,

$$A_U = 0\ \text{GeV} \quad \text{and} \quad 1\ \text{TeV}. \tag{3.13}$$

  Our lightest stop mass is hence about 400 GeV and in accordance with the LHC constraints [58].[3]
- In order to comply with the present LHC search bounds [61], we conservatively set the soft SUSY breaking masses of the squark sector of the first two generations equal to 2.5 TeV and, for simplicity, also those of the slepton sector apart from the soft SUSY breaking stau masses. The latter are chosen equal to 300 GeV. This way we still allow for rather light stau masses but are conservative enough to fulfill the latest LHC results [62]. It should be noted, however, that our results almost do not change by choosing different values in the stau sector[4] as the influence of the slepton sector on the Higgs mass corrections is negligible. And

[2] In `NMSSMTools` there is no distinction between A_u, A_c, A_t.

[3] In scenarios with a very small mass difference between the lightest stop $\tilde{t}_1$ and the lightest neutralino $\tilde{\chi}_1^0$ assumed to be the lightest SUSY particle, stop masses down to about 100–130 GeV are still allowed for $m_{\tilde{\chi}_1^0} \geqslant 90$ GeV [59,60].

[4] Also the SUSY breaking masses of the squarks of the first two generations barely influence the outcome of the scans.

contrary to the MSSM, light stau masses here do not lead to an enhancement of the partial width into photons [6], as we have chosen small values of $\tan\beta$ and $\mu_{\rm eff}$. We furthermore set the trilinear couplings of the down and lepton sector equal to 1 TeV and the right-handed soft SUSY breaking sbottom mass equal to 2.5 TeV. This results in light sbottom masses of about 500 GeV $\lesssim m_{\tilde{b}_1} \lesssim$ 800 GeV. Hence we have ($D \equiv d, s, b$, $E \equiv e, \mu, \tau$)

$$\begin{aligned} &M_{\tilde{u}_R} = M_{\tilde{c}_R} = M_{\tilde{D}_R} = M_{\tilde{Q}_{1,2}} = M_{\tilde{e}_R} = M_{\tilde{\mu}_R} = M_{\tilde{L}_{1,2}} = 2.5 \text{ TeV}, \\ &M_{\tilde{\tau}_R} = M_{\tilde{L}_3} = 300 \text{ GeV}, \qquad A_D = A_E = 1 \text{ TeV}. \end{aligned} \tag{3.14}$$

- The gluino soft SUSY breaking mass parameter has been set to

$$M_3 = 1 \text{ TeV}. \tag{3.15}$$

The remaining two soft SUSY breaking gaugino parameters have been chosen $M_1 = 150$ GeV and $M_2 = 300$ GeV.

It should be noted that in NMSSMTools the NMSSM-specific input parameters λ, κ, A_λ and A_κ according to the SLHA format are understood as running $\overline{\rm DR}$ parameters taken at the SUSY scale $\tilde{M} = 1$ TeV, while $\tan\beta$ is taken at the mass of the Z boson, M_Z.

We remark, that at the cost of a more time consuming scan we could have enlarged our parameter ranges of A_κ, A_λ and κ. As will be evident from our numerical analysis later, the limitation of the scan to this restricted parameter area nevertheless leads to a substantial amount of parameter points which are compatible with the applied constraints due to experimental results and fine-tuning arguments. Note also, that choosing large positive values for A_κ for negative κ leads to non-self-consistent solutions. Concerning A_λ, it is related to the charged Higgs boson mass, which is below the experimental limit if A_λ is chosen too small. A posteriori it also turned out that the chosen upper bound of A_λ was largely sufficient to capture the maximum of allowed parameter points which can be achieved for the chosen A_κ range.

The parameter scan is further restricted by demanding the NMSSM Higgs spectrum to fulfill the following conditions:

- We demand one of the scalar Higgs bosons, which we will denote from here on by h, to have its mass in the range

$$\underline{\text{scalar Higgs boson } h}: \quad 124 \text{ GeV} \leqslant m_h \leqslant 127 \text{ GeV}, \tag{3.16}$$

where we have conservatively assumed a 3σ error on the mass value of the scalar particle discovered at the LHC [1,2].
- In order to explore the possibility of an enhanced branching ratio into photons, we furthermore demand that the $\gamma\gamma$ rate around the invariant mass value 126 GeV fulfills:

$$\text{rate for the } \gamma\gamma \text{ final state normalised to the SM value} \gtrsim 0.8. \tag{3.17}$$

- We do not put any restrictions on the rates in the massive gauge boson and fermion final states.
- For the other Higgs bosons, *i.e.*, the pseudoscalar Higgs bosons and the scalar Higgs bosons outside the mass range around 126 GeV, we check if they have not been excluded by the LEP, Tevatron and LHC searches. Otherwise the whole parameter point is rejected. We have taken into account the newest exclusion limits in the various final states reported by the experiments [63–71], which we have implemented in NMSSMTools.

Our choice of parameters results in rather low top squark, charged Higgs boson and chargino masses, still compatible, however, with present LHC SUSY search results. For $\tan\beta = 2$ we have

$$m_{\tilde{t}_1} = 400\text{–}820\ \text{GeV}, \qquad m_{\tilde{t}_2} = 530\text{–}890\ \text{GeV}, \tag{3.18}$$

$$M_{H^\pm} = 200\text{–}500\ \text{GeV}, \qquad M_{\tilde{\chi}_1^\pm} = 105\text{–}165\ \text{GeV}, \qquad M_{\tilde{\chi}_2^\pm} = 345\text{–}360\ \text{GeV}, \tag{3.19}$$

and similar values for $\tan\beta = 4$. The stop mass values are small enough so that the fine-tuning is expected to be rather low.

We finally remark that we did not restrict our parameter points taking into account the relic density. We checked, however, that there is a substantial amount of parameter points which lead to relic densities due to a neutralino DM candidate, which are smaller than the WMAP value. To achieve the correct amount of relic density another candidate than the neutralino would have to be thought of. Furthermore, we convinced ourselves that *e.g.* by slightly changing the values of the gaugino mass parameters M_1, M_2 the correct amount of relic density could be achieved, while the Higgs mass spectrum remains practically unchanged, so that we did not further consider this constraint. For discussions taking into account DM constraints, see *e.g.* [21–24,37].

4. NMSSM Higgs boson production and decay

In order to decide whether the 126 GeV NMSSM Higgs boson reproduces the rates as measured by the experiments, its production cross sections and branching ratios have to be investigated. In the following the dominant production process through gluon fusion and its modification with respect to the SM will be discussed in detail. We furthermore investigate the NMSSM Higgs branching ratio into photons, as the LHC experiments see a slight excess here with respect to the SM. With the presently available data, this has to be taken with due caution, however, as it could still turn out to be a statistical fluctuation. If it persists, however, it is a hint towards New Physics and shall be taken into account in our analysis. We start with some preliminary remarks and set up our notation.

At the LHC, for small values of $\tan\beta$, the production processes for a single neutral CP-even NMSSM Higgs boson H_i ($i = 1, 2, 3$) or a CP-odd Higgs state A_j ($j = 1, 2$) are given by

$$\begin{aligned}
&\text{Gluon fusion:} && gg \to H_i \text{ and } gg \to A_j,\\
&\text{Gauge boson fusion:} && qq \to qq + W^*W^*/Z^*Z^* \to qqH_i,\\
&\text{Higgs-strahlung:} && q\bar{q} \to Z^*/W^* \to H_i + Z/W,\\
&\text{Associated production with } t\bar{t}\text{:} && gg/q\bar{q} \to t\bar{t}H_i \text{ and } gg/q\bar{q} \to t\bar{t}A_j,
\end{aligned} \tag{4.20}$$

where gluon fusion is the most important process followed by gauge boson fusion. Higgs-strahlung and associated production with a top quark pair[5] only play a minor role and are more important for the determination of Higgs boson couplings.

The NMSSM production processes and decay channels deviate from the corresponding SM Higgs H^{SM} processes due to modified Higgs couplings and additional SUSY particles running in the loop-mediated processes. The couplings of the CP-even Higgs states H_i (and also those of the CP-odd states) depend on their decompositions into the weak eigenstates H_d, H_u and S,

[5] For small $\tan\beta$ values associated production with a bottom quark pair is negligibly small.

$$H_1 = S_{1,d} H_d + S_{1,u} H_u + S_{1,s} S,$$
$$H_2 = S_{2,d} H_d + S_{2,u} H_u + S_{2,s} S,$$
$$H_3 = S_{3,d} H_d + S_{3,u} H_u + S_{3,s} S. \tag{4.21}$$

The coefficients $S_{i,u}, S_{i,d}$ hence quantify the amount of up- and down-likeness, respectively, while $S_{i,s}$ is a measure for the singlet component of a Higgs mass eigenstate. Mixings between the $SU(2)$-doublet and singlet sectors are proportional to λ, and can be sizeable for $\lambda \gtrsim 0.3$, leading to significant effects on the NMSSM Higgs couplings and hence phenomenology [15,16,18,19].

The inclusive production cross section σ_{incl} for a CP-even Higgs boson is composed of gluon fusion, vector boson fusion, Higgs-strahlung and associated production with $t\bar{t}$,

$$\sigma_{\text{incl}}(H) = \sigma(gg \to H) + \sigma(Hqq) + \sigma(WH) + \sigma(ZH) + \sigma(t\bar{t}H) \approx \sigma(gg \to H), \tag{4.22}$$

with $H = H_i, H^{\text{SM}}$, respectively. It is dominated by the gluon fusion cross section. For later convenience in the discussion of our results we normalise the relevant quantities of the NMSSM Higgs bosons to the corresponding SM counterparts. Thus we define the ratio $R_{\sigma_{\text{incl}}}$ of the NMSSM inclusive cross section compared to the SM one,

$$R_{\sigma_{\text{incl}}}(H_i) \equiv \frac{\sigma_{\text{incl}}(H_i)}{\sigma_{\text{incl}}(H^{\text{SM}})} \approx R_{\sigma_{gg}}(H_i), \tag{4.23}$$

where we have used $R_{\sigma_{gg}}(H_i)$ defined as the ratio of the NMSSM gluon fusion production cross section to the SM one,

$$R_{\sigma_{gg}}(H_i) \equiv \frac{\sigma(gg \to H_i)}{\sigma(gg \to H^{\text{SM}})}. \tag{4.24}$$

If not stated otherwise, in these and the following ratios the mass of the NMSSM Higgs boson H_i and the one of the SM Higgs H^{SM} are taken to be the same and they are subject to the constraint $M_{H^{\text{SM}}} = M_{H_i} \equiv m_h = 124$–$127$ GeV.

The ratio $R_{\Gamma_{\text{tot}}}$ for the total width compared to the SM Higgs total width is given by

$$R_{\Gamma_{\text{tot}}}(H_i) \equiv \frac{\Gamma_{\text{tot}}(H_i)}{\Gamma_{\text{tot}}(H^{\text{SM}})}. \tag{4.25}$$

While in the SM the largest decay width of a Higgs boson of about 126 GeV is the one into bb, the most important search channels are given by the $\gamma\gamma$, the massive gauge boson and the $\tau\tau$ final states. We define the ratios of the NMSSM Higgs decay partial widths relative to the SM as $(X = \gamma, W, Z, b, \tau)$

$$R_{\Gamma_{XX}}(H_i) \equiv \frac{\Gamma(H_i \to XX)}{\Gamma(H^{\text{SM}} \to XX)}. \tag{4.26}$$

The ratios of branching ratios are given by

$$R^{BR}_{XX}(H_i) \equiv \frac{BR(H_i \to XX)}{BR(H^{\text{SM}} \to XX)} = \frac{R_{\Gamma_{XX}}(H_i)}{R_{\Gamma_{\text{tot}}}(H_i)}. \tag{4.27}$$

The experimentally observed rate in a given channel X is given by the reduced cross section R_{XX} which is obtained from multiplying the Higgs production ratio relative to the SM, $R_{\sigma_{\text{incl}}}(H_i)$, with the Higgs branching ratio for the channel of interest relative to the SM. For example, for the two photon final state we have

$$R_{\gamma\gamma}(H_i) \equiv R_{\sigma_{\rm incl}}(H_i) R^{BR}_{\gamma\gamma}(H_i). \tag{4.28}$$

The corresponding reduced cross sections in the other decay channels VV ($V = W, Z$), bb, $\tau\tau$ may be similarly expressed, namely:

$$\begin{aligned} &R_{VV}(H_i) \equiv R_{\sigma_{\rm incl}}(H_i) R^{BR}_{VV}(H_i), \qquad R_{bb}(H_i) \equiv R_{\sigma(VH)}(H_i) R^{BR}_{bb}(H_i), \\ &R_{\tau\tau}(H_i) \equiv R_{\sigma_{\rm incl}}(H_i) R^{BR}_{\tau\tau}(H_i). \end{aligned} \tag{4.29}$$

In the bb final state we restrict ourselves to associated production of the Higgs boson with a W or Z boson, as we will compare our results later with values given for this channel by the experiments.

It is important to note that there can be NMSSM spectra where two neutral Higgs bosons lie close in mass. Due to the limited experimental resolution these cannot be separated from each other and both contribute to the signal. The program `NMSSMTools` takes this into account by super-imposing the signal from the nearby Higgs boson with a Gaussian weighting. The width of the Gaussian smearing is adapted to the respective experimental resolution in the different final states, where clearly the $\gamma\gamma$ and ZZ final states have the best resolution, while the mass resolution in the $\tau\tau$ and bb final states is less good, and in the WW final state the mass cannot be reconstructed. Hence, the ratios for the rates, R_{XX}, depending on the scenario and related NMSSM spectrum under consideration, can be superpositions of rates of different Higgs bosons. In favour of an unambiguous notation and to make contact with the signal strengths $\mu = \sigma/\sigma_{\rm SM}$ reported by the LHC experiments, we denote by μ_{XX} the reduced cross sections (4.28), (4.29), which are built up by the superposition of the rates from the 126 GeV h boson and another Higgs boson $\Phi = H_i, A_j$, which has a mass close to 126 GeV,

$$\mu_{XX}(h) \equiv R_\sigma(h) R^{BR}_{XX}(h) + \sum_{\substack{\Phi \neq h \\ |M_\Phi - M_h| \leqslant \delta}} R_\sigma(\Phi) R^{BR}_{XX}(\Phi) F(M_h, M_\Phi, d_{XX}). \tag{4.30}$$

Here $\sigma = \sigma(VH)$, $H = h, \Phi$, in case $X = b$ and $\sigma = \sigma_{\rm incl}$ otherwise. By δ we denote the mass resolution in the respective XX final state and by $F(M_h, M_\Phi, d_{XX})$ the Gaussian weighting function as implemented in `NMSSMTools`. The experimental resolution of the different channels is taken into account by the parameter d_{XX}, which influences the width of the weighting function. We impose the restriction (3.17) on the thus calculated $\gamma\gamma$ rate, which in fact is the one observed in experiment. Hence, in summary the conditions we impose on our parameter points are:

Conditions on the parameter scan:

At least one CP-even Higgs boson h with: $\quad 124\ {\rm GeV} \lesssim M_h \lesssim 127\ {\rm GeV}$,

The reduced cross section for $\gamma\gamma$ must fulfill:

$$\mu_{\gamma\gamma}(h) \gtrsim 0.8 \quad \text{with } 124\ {\rm GeV} \lesssim M_h = M_{H^{\rm SM}} \lesssim 127\ {\rm GeV}. \tag{4.31}$$

4.1. Higgs boson production through gluon fusion

The cross section for NMSSM Higgs production via gluon fusion is mediated by quark Q and squark $\tilde{Q}$ triangle loops, *cf.* Fig. 1. The latter become particularly important for squark masses below about 400 GeV [4,5,9,72]. At leading order (LO) in the narrow-width approximation the hadronic cross section for scalar Higgs bosons H_i ($i = 1, 2, 3$) can be cast into the form [72–74]

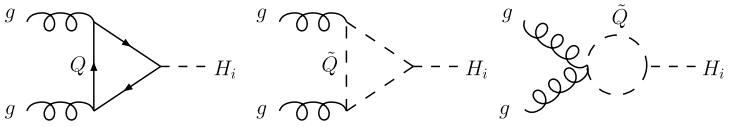

Fig. 1. Generic diagrams contributing gluon fusion production of H_i.

$$\sigma_{\rm LO}(pp \to H_i) = \sigma_0^{H_i} \tau_{H_i} \frac{d\mathcal{L}^{gg}}{d\tau_{H_i}}, \tag{4.32}$$

$$\sigma_0^{H_i} = \frac{G_F \alpha_s^2(\mu_R)}{288\sqrt{2}\pi} \left| \sum_Q g_Q^{H_i} A_Q^{H_i}(\tau_Q) + \sum_{\tilde{Q}} g_{\tilde{Q}}^{H_i} A_{\tilde{Q}}^{H_i}(\tau_{\tilde{Q}}) \right|^2, \tag{4.33}$$

with the gluon luminosity $\mathcal{L}_{gg}$, the Fermi constant G_F, $\tau_{H_i} = M_{H_i}^2/s$, where s denotes the squared hadronic c.m. energy and $\tau_X = 4M_X^2/M_{H_i}^2$ ($X = Q, \tilde{Q}$). The strong coupling constant α_s is taken at the scale μ_R chosen equal to the mass of H_i. The form factors $A_{Q/\tilde{Q}}^{H_i}$ are given by

$$A_Q^{H_i}(\tau) = \frac{3}{2}\tau\big[1 + (1-\tau) f(\tau)\big], \tag{4.34}$$

$$A_{\tilde{Q}}^{H_i}(\tau) = -\frac{3}{4}\tau\big[1 - \tau f(\tau)\big] \tag{4.35}$$

and the function $f(\tau)$ reads

$$f(\tau) = \begin{cases} \arcsin^2 \frac{1}{\sqrt{\tau}} & \tau \geqslant 1, \\ -\frac{1}{4}[\log \frac{1+\sqrt{1-\tau}}{1-\sqrt{1-\tau}} - i\pi]^2 & \tau < 1. \end{cases} \tag{4.36}$$

For large values of the loop particle masses the form factors become constant,

$$A_Q^{H_i}(\tau) \to 1 \quad \text{for } M_{H_i}^2 \ll 4m_Q^2, \tag{4.37}$$

$$A_{\tilde{Q}}^{H_i}(\tau) \to \frac{1}{4} \quad \text{for } M_{H_i}^2 \ll 4m_{\tilde{Q}}^2. \tag{4.38}$$

For small values of $\tan\beta$ the most important contributions come from the top and stop loops. In order to study the effect of the stop loops and their interplay with the top quark loop, the Higgs couplings to the top and stop quarks, $g_Q^{H_i}$, $g_{\tilde{Q}}^{H_i}$, have to be investigated. Due to the diagonal gluon coupling to stops, in the loop only the Higgs couplings to two equal stops can appear. Hence for $g_{\tilde{Q}}^{H_i}$ we have to consider the couplings

$$\begin{aligned} g_{H_i\tilde{t}_1\tilde{t}_1} = {} & (S_{i,d}\cos\beta - S_{i,u}\sin\beta)\frac{M_Z^2}{m_{\tilde{t}_1}^2}\left(\frac{1}{2}\cos^2\theta_{\tilde{t}} - \frac{2}{3}\sin^2\theta_W\cos 2\theta_{\tilde{t}}\right) + \frac{m_t^2 S_{i,u}}{m_{\tilde{t}_1}^2 \sin\beta} \\ & + \frac{1}{2}\sin 2\theta_{\tilde{t}}\frac{m_t}{m_{\tilde{t}_1}^2 \sin\beta}\left[-\mu_{\rm eff} S_{i,d} + A_t S_{i,u} - \frac{\lambda v \cos\beta}{\sqrt{2}} S_{i,s}\right], \end{aligned} \tag{4.39}$$

$$\begin{aligned} g_{H_i\tilde{t}_2\tilde{t}_2} = {} & (S_{i,d}\cos\beta - S_{i,u}\sin\beta)\frac{M_Z^2}{m_{\tilde{t}_2}^2}\left(\frac{1}{2}\sin^2\theta_{\tilde{t}} + \frac{2}{3}\sin^2\theta_W\cos 2\theta_{\tilde{t}}\right) + \frac{m_t^2 S_{i,u}}{m_{\tilde{t}_2}^2 \sin\beta} \\ & - \frac{1}{2}\sin 2\theta_{\tilde{t}}\frac{m_t}{m_{\tilde{t}_2}^2 \sin\beta}\left[-\mu_{\rm eff} S_{i,d} + A_t S_{i,u} - \frac{\lambda v \cos\beta}{\sqrt{2}} S_{i,s}\right]. \end{aligned} \tag{4.40}$$

The Higgs mixing matrix elements $S_{i,x}$ $(x = d, u, s)$ have been defined in Eq. (4.21). We are interested in NMSSM parameter scenarios with one of the CP-even Higgs bosons having a mass around 126 GeV and production rates which are not too far away from the corresponding SM rates in the various final states in order to comply with the LHC Higgs search results. For the sake of simplicity in the investigation of the couplings we therefore define the SM limit of the NMSSM, which is given by first performing the MSSM limit, which is recovered by $\lambda, \kappa \to 0$ with κ/λ constant and keeping the parameters μ_{eff}, A_λ and A_κ fixed. Within the MSSM limit then the decoupling limit is performed. In the thus defined SM limit the mixing matrix elements of h become

$$S_{i,d} \to \cos\beta, \qquad S_{i,u} \to \sin\beta, \qquad S_{i,s} \to 0. \tag{4.41}$$

And we get for the couplings to the stops

$$\begin{aligned} g^{\text{SM}}_{h\tilde{t}_1\tilde{t}_1} &= \cos 2\beta \frac{M_Z^2}{m^2_{\tilde{t}_1}} \left(\frac{1}{2}\cos^2\theta_{\tilde{t}} - \frac{2}{3}\sin^2\theta_W \cos 2\theta_{\tilde{t}} \right) + \frac{m_t^2}{m^2_{\tilde{t}_1}} \\ &\quad + \frac{1}{2}\sin 2\theta_{\tilde{t}} \frac{m_t}{m^2_{\tilde{t}_1}\sin\beta}[-\mu_{\text{eff}}\cos\beta + A_t \sin\beta], \end{aligned} \tag{4.42}$$

$$\begin{aligned} g^{\text{SM}}_{h\tilde{t}_2\tilde{t}_2} &= \cos 2\beta \frac{M_Z^2}{m^2_{\tilde{t}_2}} \left(\frac{1}{2}\sin^2\theta_{\tilde{t}} + \frac{2}{3}\sin^2\theta_W \cos 2\theta_{\tilde{t}} \right) + \frac{m_t^2}{m^2_{\tilde{t}_2}} \\ &\quad - \frac{1}{2}\sin 2\theta_{\tilde{t}} \frac{m_t}{m^2_{\tilde{t}_2}\sin\beta}[-\mu_{\text{eff}}\cos\beta + A_t \sin\beta]. \end{aligned} \tag{4.43}$$

In the scenarios of the parameter scan which are left over after applying our criteria (4.31), for $\tan\beta = 2$ the relations (4.41) are approximately fulfilled apart from the singlet component, which can take values of up to $\sim$0.1. The approximation gets worse in scenarios with strong singlet–doublet mixing, where the singlet component can reach values of up to $\sim$0.6. In this case we can have suppressed couplings of the 126 GeV Higgs boson to bottom quarks. For $\tan\beta = 4$ the behaviour is similar for large mixing, while for small mixing the deviations from this SM limit are more important. Note, that suppressed couplings to top quarks are largely ruled out due to our demand of the $\gamma\gamma$ reduced cross section exceeding 80% of the SM value. This can only be achieved if the dominant production cross section through gluon fusion is large enough, which is not the case for Higgs couplings to the top quarks being too suppressed compared to the SM value. Nevertheless, also the top quark couplings can be suppressed compared to the SM in the cases where the branching ratio into $\gamma\gamma$ is enhanced or where the Higgs rates are built up by the superposition of rates stemming from more than one Higgs boson, so that our restriction on the $\gamma\gamma$ rate can be fulfilled.

The mixing angle $\theta_{\tilde{t}}$ which diagonalises the stop mass matrix is given by

$$\sin 2\theta_{\tilde{t}} = \frac{2m_t(A_t - \mu_{\text{eff}}/\tan\beta)}{m^2_{\tilde{t}_1} - m^2_{\tilde{t}_2}}, \tag{4.44}$$

where $m_{\tilde{t}_{1\,(2)}}$ denotes the lighter (heavier) stop quark mass. For the sake of the discussion we assume μ_{eff} to be zero.[6] With this approximation and neglecting small D-term contributions we

[6] Our values of μ_{eff} are small enough not to change the conclusions for non-zero values.

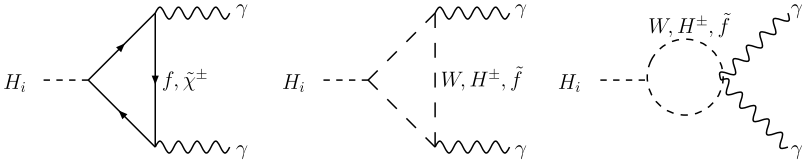

Fig. 2. Generic diagrams contributing to the decay $H_i \to \gamma\gamma$.

have for $M_{\tilde{Q}_3} = M_{\tilde{t}_R}$ the mass difference $m^2_{\tilde{t}_2} - m^2_{\tilde{t}_1} = 2m_t A_t$. For large values of A_t, the m_t^2-term and the last term in (4.42) therefore have opposite sign (in (4.43) same sign). Neglecting the small D-term contribution given by the first term in the coupling, the Higgs coupling to the lighter stops $\tilde{t}_1$ becomes negative in this case. Assuming $\tilde{t}_1$ to be relatively light, the contribution from the $\tilde{t}_1$ loop will be more important and we will not consider the $\tilde{t}_2$ loop contribution in this case. The H_i coupling to the top quarks on the other hand is given by

$$g_Q^{H_i} \equiv g_{H_i tt} = \frac{S_{i,u}}{\sin\beta}, \tag{4.45}$$

which becomes in the SM limit for the 126 GeV Higgs boson

$$g_{htt} = 1. \tag{4.46}$$

Hence for large values of A_t the $\tilde{t}_1$ and the top loop contributions interfere destructively so that the gluon fusion cross section decreases. For small values of A_t there is no mixing in the stop sector leading to a positive Higgs coupling to $\tilde{t}_1$ and constructive interference, thus enhancing the gluon fusion production cross section. For non-zero intermediate A_t values, the last two contributions of (4.42) cancel each other (the exact value of A_t depends on the specific parameter choices), and the stop contribution is small.[7] The Higgs coupling values to the sbottoms are hardly influenced by a change in A_t which enters in the mixing matrix elements $S_{i,x}$ only through higher order corrections to the Higgs boson masses.

4.2. Higgs decay width into two photons

The decays of the scalar NMSSM Higgs bosons into photons are mediated by W boson and heavy fermion loops as in the Standard Model and, in addition, by charged Higgs boson, sfermion and chargino loops; the relevant diagrams are shown in Fig. 2. The partial decay widths, adapted from the MSSM result [72,74,75], are given by

$$\begin{aligned}\Gamma(H_i \to \gamma\gamma) = \frac{G_F \alpha^2 M_{H_i}^3}{128\sqrt{2}\pi^3} \Bigg| & \sum_f N_{\rm cf} e_f^2 g_f^{H_i} A_f^{H_i}(\tau_f) + g_W^{H_i} A_W^{H_i}(\tau_W) + g_{H^\pm}^{H_i} A_{H^\pm}^{H_i}(\tau_{H^\pm}) \\ & + \sum_{\tilde{\chi}^\pm} g_{\tilde{\chi}^\pm}^{H_i} A_{\tilde{\chi}^\pm}^{H_i}(\tau_{\tilde{\chi}^\pm}) + \sum_{\tilde{f}} N_{\rm cf} e_{\tilde{f}}^2 g_{\tilde{f}}^{H_i} A_{\tilde{f}}^{H_i}(\tau_{\tilde{f}}) \Bigg|^2, \end{aligned} \tag{4.47}$$

with the colour factor $N_{\rm cf} = 1$ (3) for leptons (quarks) and e_f denoting the electric charge of the loop particle. The form factors are given by

[7] The influence of the stop loop contributions on gluon fusion and decay into photon final states has been discussed in the context of the MSSM in detail in [5].

$$A^{H_i}_{f,\tilde{\chi}^\pm}(\tau) = 2\tau\big[1 + (1-\tau) f(\tau)\big], \tag{4.48}$$

$$A^{H_i}_{H^\pm,\tilde{f}}(\tau) = -\tau\big[1 - \tau f(\tau)\big], \tag{4.49}$$

$$A^{H_i}_{W}(\tau) = -\big[2 + 3\tau + 3\tau(2-\tau) f(\tau)\big], \tag{4.50}$$

where $\tau = 4M_X^2/M_{H_i}^2$ with M_X being the mass of the particle X in the loop. For large loop particle masses M_X the form factors approach constant values,

$$\begin{aligned} A^{H_i}_{f,\tilde{\chi}^\pm}(\tau) &\to \frac{4}{3} \quad \text{for } M_{H_i}^2 \ll 4M_{f,\tilde{\chi}^\pm}^2, \\ A^{H_i}_{H^\pm,\tilde{f}}(\tau) &\to \frac{1}{3} \quad \text{for } M_{H_i}^2 \ll 4M_{H^\pm,\tilde{f}}^2, \\ A^{H_i}_{W}(\tau) &\to -7 \quad \text{for } M_{H_i}^2 \ll 4M_{W}^2. \end{aligned} \tag{4.51}$$

The Higgs couplings to fermions, W bosons, charged Higgs bosons and charginos, appearing in the decay width into two photons, are given by

$$g^{H_i}_f = \begin{cases} S_{i,u}/\sin\beta & \text{for } f = \text{up-type fermion}, \\ S_{i,d}/\cos\beta & \text{for } f = \text{down-type fermion}, \end{cases} \tag{4.52}$$

$$g^{H_i}_W = S_{i,d}\cos\beta + S_{i,u}\sin\beta, \tag{4.53}$$

$$g^{H_i}_{\tilde{\chi}^\pm} \equiv g^{H_i}_{\tilde{\chi}_k^\pm \tilde{\chi}_k^\mp} = \frac{2M_W}{M_{\tilde{\chi}_k^\pm}}[q_{kk} S_{i,d} + s_{kk} S_{i,u} + r_{kk} S_{i,s}], \tag{4.54}$$

$$\begin{aligned} g^{H_i}_{H^\pm} = \frac{M_W^2}{M_{H^\pm}^2}\Bigg[& \frac{\cos(2\theta_W)}{2\cos^2\theta_W}\big(\cos^3\beta S_{i,d} + \sin^3\beta S_{i,u}\big) \\ & + \frac{1}{2}\cos\beta\sin\beta\big(\big(3 + \tan^2\theta_W\big) - 4\lambda^2/g^2\big)(\sin\beta S_{i,d} + \cos\beta S_{i,u}) \\ & + \frac{1}{\sqrt{2} g M_W}\big(2\lambda\mu_{\text{eff}} + \sin 2\beta(A_\lambda\lambda + 2\kappa\mu_{\text{eff}})\big) S_{i,s}\Bigg]. \end{aligned} \tag{4.55}$$

The matrix elements q_{kl}, s_{kl}, r_{kl} $(k,l = 1,2)$ in terms of the matrix elements of the matrices U, V diagonalising the chargino mass matrix [76] read

$$q_{kl} = \frac{1}{\sqrt{2}} U_{l2} V_{k1}, \qquad s_{kl} = \frac{1}{\sqrt{2}} U_{l1} V_{k2}, \qquad r_{kl} = \frac{\lambda v}{2\sqrt{2} M_W} U_{l2} V_{k2}. \tag{4.56}$$

In the SM limit, defined in the previous subsection, the couplings become

$$g^{H_i}_f \to 1, \tag{4.57}$$

$$g^{H_i}_W \to 1, \tag{4.58}$$

$$g^{H_i}_{H^\pm} \to \frac{M_W^2}{M_{H^\pm}^2}\left[\frac{\cos(2\theta_W)}{2\cos^2\theta_W}\big(\cos^4\beta + \sin^4\beta\big) + \cos^2\beta\sin^2\beta\left(\big(3 + \tan^2\theta_W\big) - 4\frac{\lambda^2}{g^2}\right)\right], \tag{4.59}$$

$$g^{H_i}_{\tilde{\chi}_k^\pm \tilde{\chi}_k^\pm} \to \frac{2M_W}{M_{\tilde{\chi}_k^\pm}}(q_{kk}\cos\beta + s_{kk}\sin\beta). \tag{4.60}$$

The sfermion loop contributions are only important for the third generation with light masses. While it has been shown in the context of the MSSM that the $\tilde{\tau}$ loop contributions can enhance the decay width into photons [6], this is not the case here as we assume small values of $\tan\beta$ and $\mu_{\rm eff}$. Due to the small $\tan\beta$ values also sbottom loops play a minor role. The most important sfermion contribution comes from the stop loops in particular a light $\tilde{t}_1$. The Higgs coupling to the stops has been given in Section 4.1, Eqs. (4.39), (4.40) and for the SM limit in Eqs. (4.42), (4.43). Since in the Higgs decay into photons the quark and W loop contributions interfere destructively, in the decay the effect of the stop loops is opposite to the one in the production. For $A_t = 0$ GeV the stop loop contribution suppresses the decay into photons, for $A_t = 1$ TeV it leads to an enhancement.

For light enough chargino and charged Higgs boson masses their loop contribution also plays a role. We find that they can lead to an enhancement for the partial decay width into photons (see also [7,12,13]).

5. Numerical analysis

In this section we show our numerical results. When performing the scans we find scenarios in which both the lightest scalar Higgs H_1 and the heavier one H_2 can have masses around 126 GeV. We will call the respective Higgs boson in this case h. Not all its couplings are necessarily equal or near the corresponding SM Higgs coupling values. More importantly the reduced cross sections in the various final states, which can be superpositions of signals from Higgs bosons with masses close to 126 GeV, as defined in Eq. (4.30), have to reproduce the experimental results. To avoid a flood of plots, in the following we will only show the ones for $\tan\beta = 2$ and comment on the plots for $\tan\beta = 4$.

5.1. Parameter values and mass distributions

In Fig. 3 we show the distributions of the allowed parameter points in the κ–λ plane leading to H_1 representing the CP-even Higgs boson with mass in the range 124–127 GeV (left) and to H_2 (right) being h, respectively, for the two values of $A_t = 0$ GeV and 1 TeV. The colour code denotes the number of points. As can be inferred from the figures, we have much more points allowing for $h = H_2$ than for $h = H_1$. This can be explained as follows. As we demand the stop mass parameters to be rather low, which leads to smaller higher order corrections for a fixed mixing, the parameter λ at low energies must be large enough to get to the right mass. The demand of perturbativity up to the GUT scale then implies stringent constraints on the coupling κ(1 TeV). In addition $\mu_{\rm eff}$ is required to be smaller than 200 GeV to avoid fine-tuning. Because the masses of the extra NMSSM scalar and pseudoscalar states, which are predominantly SM singlets, are set by $\kappa\mu_{\rm eff}/\lambda$ these states tend to be lighter than the 126 GeV Higgs boson. As both the H_1 and H_2 mass values increase with rising κ, for H_1 we need for the same reasons large κ values of $\kappa \approx 0.4$, while too large values of κ lead to too large H_2 masses so that here values $\kappa \approx 0.07$–0.09 are preferred. With increasing values of A_t the stop mass corrections to the tree-level masses become more important so that a 126 GeV Higgs mass can be attained more easily and therefore more parameter points pass the constraints. For the same reason the maximum of points is given for smaller values of λ now, decreasing from $\lambda \approx 0.73\,(0.72)$ at small stop mixing to $\lambda \approx 0.68\,(0.66)$ for $h = H_1\,(H_2)$ at large mixing.

In the plots we also show the upper bounds on λ and κ imposed by perturbativity derived from the two-loop renormalisation group running from the GUT scale down to 1 TeV. These

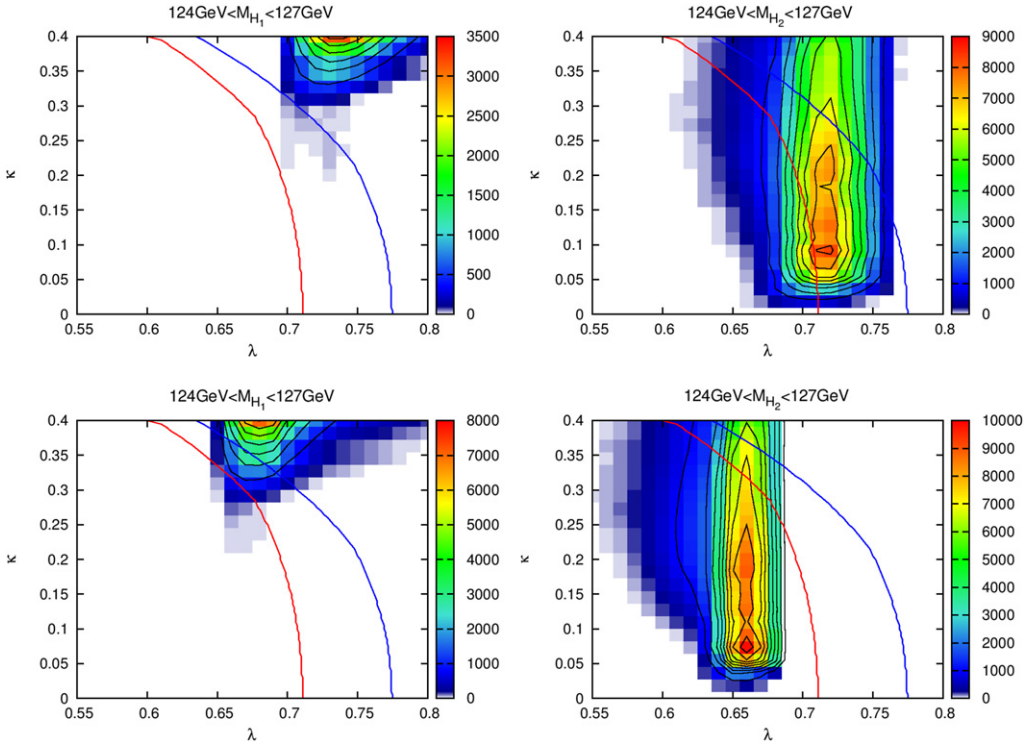

Fig. 3. The distribution of allowed parameter points in the κ–λ plane for $h = H_1$ (left) and $h = H_2$ (right) for $A_t = 0$ GeV (upper) and $A_t = 1$ TeV (lower). The red (blue) contour lines show the two-loop upper bounds for λ and κ at 1 TeV in the NMSSM without (with) extra matter above 1 TeV. The colour code denotes the number of points. (For interpretation of the references to colour in this figure legend, the reader is referred to the web version of this article.)

limits can be somewhat relaxed when allowing for extra exotic matter with mass around 1 TeV. They show that an H_1 Higgs boson with mass around 126 GeV can only be achieved for large mixing with $A_t = 1$ TeV. For lower values of A_t even with the inclusion of extra matter, this is not possible. The heavier Higgs boson H_2 on the other hand can have a 126 GeV mass value with and without exotic matter. We finally note that in case $A_t = 0$ GeV, for $h = H_1$ the trilinear couplings A_κ, A_λ cluster around $(A_\kappa, A_\lambda) = (0\text{ GeV}, 310\text{ GeV})$ and for $h = H_2$ around $(A_\kappa, A_\lambda) = (-140\text{ GeV}, 310\text{ GeV})$. In case $A_t = 1$ TeV, we have for $h = H_1$ the maximum of points around $(A_\kappa, A_\lambda) = (0\text{ GeV}, 340\text{ GeV})$ and for $h = H_2$ around $(A_\kappa, A_\lambda) = (-140\text{ GeV}, 340\text{ GeV})$.

Fig. 4 shows the mass distributions of the lighter neutral Higgs bosons for H_1 and H_2 being h, respectively. For $h = H_1$ there exist parameter regions where H_2 and/or A_1 are very close in mass. Depending on the respective experimental resolution in the investigated final state their signal can superimpose the h rate. This superposition has been taken into account in the reduced cross sections discussed later. The maximum of parameter points clusters around mass values $M_{H_2,A_1} \approx (175, 170)$ GeV. Also for H_2 with mass $\sim$126 GeV the H_1 and/or A_1 state can be close in mass and contribute to the signal. Their masses can be also much smaller, however, so that H_2 decays into these final states become possible, leading to distinct signatures [77]. The maximum parameter points are found for $M_{H_1,A_1} \approx (85, 110)$ GeV. The masses of the heavier Higgs bosons H_3 and A_2 lie between about 300 and 500 GeV.

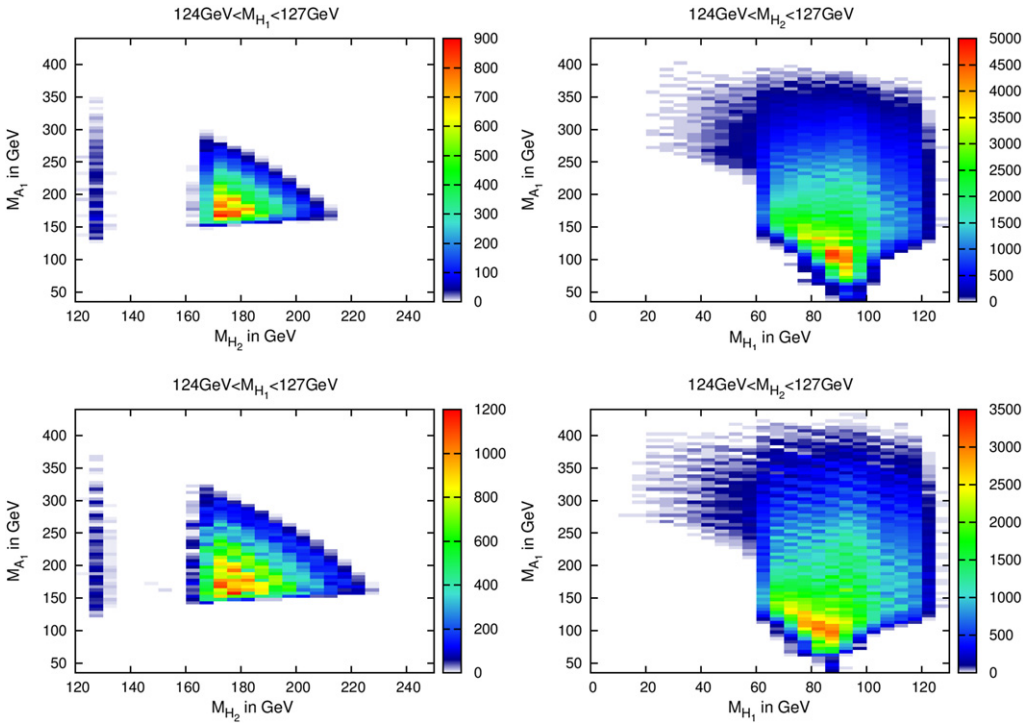

Fig. 4. Mass spectrum of A_1 and H_2 for $h = H_1$ (left) and of A_1 and H_1 for $h = H_2$ (right) with $A_t = 0$ GeV (upper) and 1 TeV (lower). The colour code denotes the number of points. (For interpretation of the references to colour in this figure legend, the reader is referred to the web version of this article.)

We remind the reader that in all plots we have already taken into account the latest exclusion limits from LEP, Tevatron and LHC which apply to the non-h Higgs bosons. In particular for scenarios with $h = H_1$ this leads to a substantial reduction of allowed parameter points.

As for $\tan\beta = 4$, it turns out that for small mixing no parameter combination fulfills the conditions (4.31) for the lightest NMSSM Higgs boson H_1. Only for large mixing a few hundred parameter points survive which cluster around $(\kappa, \lambda) = (0.4, 0.8)$. For $h = H_2$ both in the low and in the large mixing case the conditions are fulfilled with the maximum of points in a somewhat extended region around $(\kappa, \lambda) = (0.4, 0.8)$. The reason is that for larger values of $\tan\beta$ the tree-level upper mass bound is lower than for $\tan\beta = 2$, so that more substantial higher order mass corrections are needed which in case H_1 is to have a mass around 126 GeV can be achieved only for large mixing. If we now apply the perturbativity bounds on κ and λ it turns out, however, that none of the $h = H_1$ scenarios survives as even with extra matter at 1 TeV the maximum allowed value is $\lambda = 0.66$ for $\kappa = 0.4$. For the $h = H_2$ scenarios a few scenarios survive if extra matter is included. Otherwise the perturbativity bounds imposing a maximum value $\lambda = 0.64$ for $\kappa = 0.4$ are not respected.

We summarise, that for $\tan\beta = 2$ there are scenarios with $h = H_1$ which respect perturbativity in case of large mixing and inclusion of extra matter at 1 TeV. For $h = H_2$ this is the case for both small and large mixing and NMSSM with and without extra matter. For $\tan\beta = 4$ only $h = H_2$ scenarios survive and are compatible with perturbativity for low and large mixing if extra matter is included.

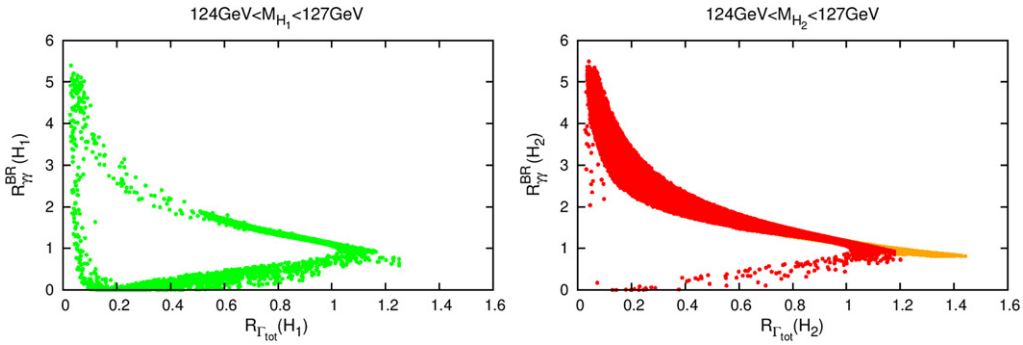

Fig. 5. Branching ratio into $\gamma\gamma$ relative to the SM against the normalised total width for $h = H_1$ (left) and $h = H_2$ (right) and $A_t = 1$ TeV. The orange points (for $h = H_2$) indicate that non-SM decays are allowed. (For interpretation of the references to colour in this figure legend, the reader is referred to the web version of this article.)

5.2. *The $\gamma\gamma$ final state*

We first discuss the behaviour of the photonic branching ratio, which is shown in Fig. 5 with respect to the SM compared to the normalised total width for $h = H_1$ and H_2, respectively, and $A_t = 1$ TeV. The plots for $A_t = 0$ GeV look very similar and therefore are not shown here. The branching ratio into $\gamma\gamma$ can be largely enhanced up to $\sim$5.6 times the SM value. This is due to a substantially suppressed total width because of strong singlet–doublet mixing of the Higgs boson with mass $\sim$126 GeV. Its coupling to bottom quarks is therefore strongly reduced, leading to a small total width (dominated by the decay into b quarks) and hence an enhanced branching ratio. The increase in the branching ratio, however, can also be due to an enhanced decay width into photons caused by squark, charged Higgs and/or chargino loop contributions, as has been discussed above. Therefore also for enhanced total widths the branching ratio can be larger than in the SM case. If, however, besides the couplings to bottom quarks also the other Higgs couplings are substantially suppressed due to strong singlet–doublet mixing, the loop-induced coupling to photons becomes very small, leading to small branching ratios also in the case of small total widths. For $h = H_2$ we can observe that the total width can be increased by up to $\sim$1.5 compared to the SM. This happens where decays of H_2 into other lighter Higgs bosons H_1 or A_1 and/or neutralino final states are kinematically allowed [77]. The relevant decays are $H_2 \to \tilde{\chi}_1^0 \tilde{\chi}_1^0$, $H_2 \to H_1 H_1$ and $H_2 \to A_1 A_1$, with the latter being rarely realised.

The corresponding plots to Fig. 5 for $\tan\beta = 4$ show a similar behaviour with altogether less parameter points, however, and a maximum photonic branching ratio enhancement of $R_{\gamma\gamma} \approx 5$ for both $h = H_2$ and H_1 (with only the large mixing case surviving here). And for the total width the maximum value is $R_{\Gamma_{\text{tot}}} \approx 1.35$ due to H_2 decays into light Higgs bosons or neutralinos.

With Fig. 6 we discuss the interplay of production and decay on the photon rate. We show the branching ratio into $\gamma\gamma$ relative to the SM plotted against the inclusive cross section normalised to the SM for either $h = H_1$ or $h = H_2$. As the inclusive production is dominated by gluon fusion, we can restrict our discussion to this production process. The figures show that for vanishing A_t gluon fusion can indeed be enhanced compared to the SM due to stop loop contributions, as has been discussed in Section 4.1. With rising mixing the stop loop contribution interferes destructively, and for $A_t = 1$ TeV the gluon fusion process is suppressed compared to the SM. Also the branching ratio into photons shows the expected opposite behaviour. For large values

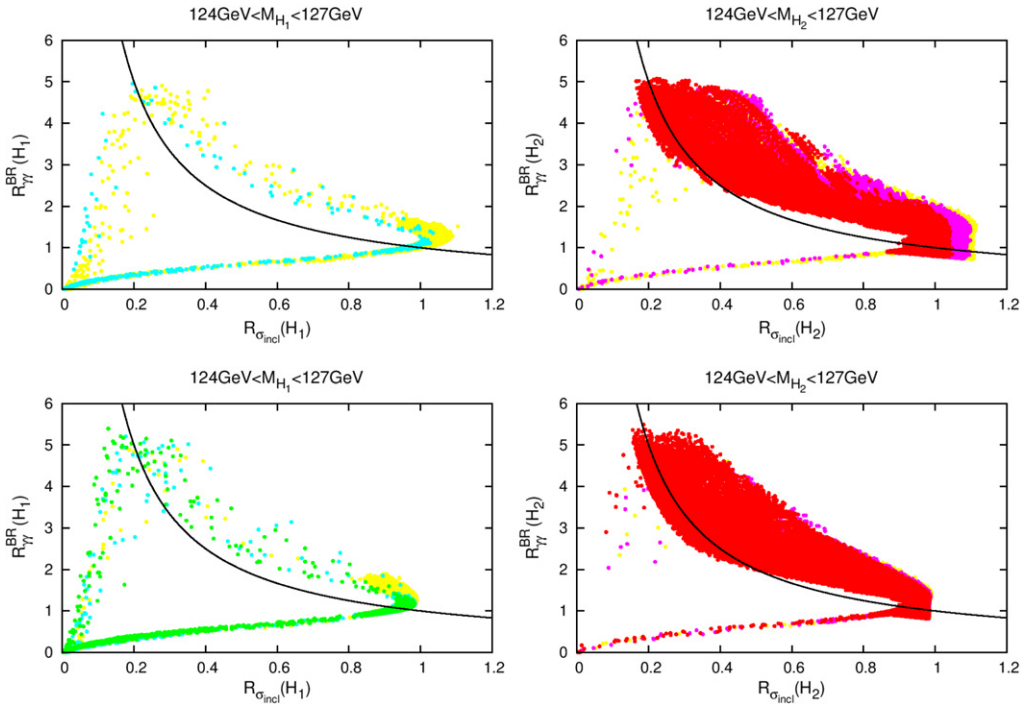

Fig. 6. Branching ratio into $\gamma\gamma$ relative to the SM against the inclusive production cross section relative to the SM for $h = H_1$(left) and $h = H_2$(right) for $A_t = 0$ GeV (upper) and $A_t = 1$ TeV (lower). For green/red points the perturbation theory is valid up to the GUT scale. Cyan/pink points require extra matter above 1 TeV and yellow points violate the two-loop upper bounds on λ, κ both with and without extra matter. Points above the black line lead to an enhanced $R_{\gamma\gamma}$. (For interpretation of the references to colour in this figure legend, the reader is referred to the web version of this article.)

of A_t, where constructively interfering stop loops enhance the partial width, we can observe slightly larger branching ratios than for $A_t = 0$ GeV. It should be kept in mind though that the behaviour of the branching ratio is an interplay of the partial width into photons and the total width. Once again for $\tan\beta = 4$ the corresponding plots to Fig. 6 show a similar behaviour with altogether less parameters points.

Above the black line the reduced cross section $R_{\gamma\gamma} = R^{BR}_{\gamma\gamma} R_{\sigma_{\rm incl}} \geqslant 1$.[8] As can be inferred from the plots, in the NMSSM both H_1 and H_2 are compatible with a 126 GeV Higgs boson and an enhanced rate into photon final states. For $h = H_2$ there are substantially more (red) points, which are compatible with the constraints that come from the requirement of the validity of the perturbation theory up to the GUT scale, than for $h = H_1$ (green points). In particular for vanishing A_t extra matter is required, behaviour which can be traced back to the need of the H_1 tree-level mass being as large as possible, *cf.* the discussion in the previous subsection. We note that there are scenarios where both the branching ratio and the inclusive production are very small due to h being very singlet-like. These scenarios passed the constraint (4.31) as in this

[8] Note that we discuss here the reduced cross section for h only. Later we will look at reduced cross sections μ_{XX} in the final state X, built up by the 126 GeV Higgs boson and possibly nearby Higgs resonances. This is what actually is observed in the experiment.

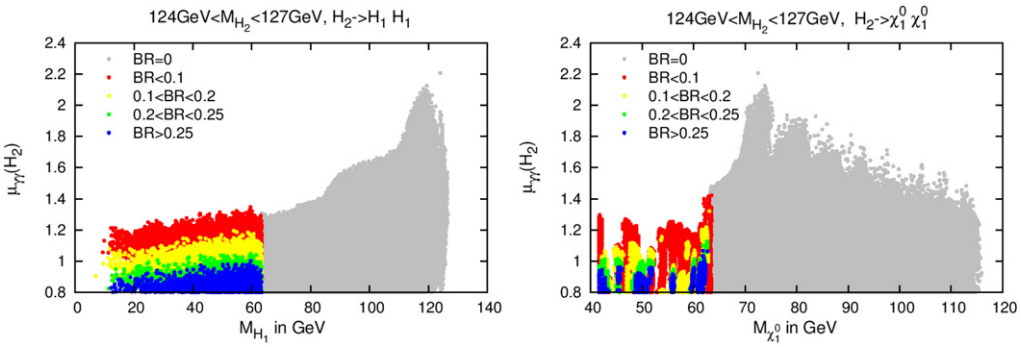

Fig. 7. Reduced cross sections into $\gamma\gamma$ against M_{H_1} (left) and $M_{\tilde{\chi}_1^0}$ (right) for $h = H_2$, $\tan\beta = 2$ and $A_t = 1$ TeV. The colour code denotes the size of the branching ratio $BR(H_2 \to H_1 H_1)$ (left) and $BR(H_2 \to \tilde{\chi}_1^0 \tilde{\chi}_1^0)$ (right). (For interpretation of the references to colour in this figure legend, the reader is referred to the web version of this article.)

case the photon reduced cross section $\mu_{\gamma\gamma}$, which can be a superposition of contributions from various Higgs bosons being close in mass, is dominated by the contribution from another light Higgs boson with a mass of ∼126 GeV, which is not singlet-like in this case.

As already mentioned above the heavier CP-even Higgs boson H_2 can decay into a pair of lighter Higgs bosons or neutralinos in certain parameter regions. This is shown in Fig. 7, where for $\tan\beta = 2$ and $A_t = 1$ TeV the reduced cross section in the $\gamma\gamma$ final state in case of $h = H_2$, $\mu_{\gamma\gamma}(H_2)$, is plotted against the mass of the lightest scalar Higgs boson H_1 and the mass of the lightest neutralino $\tilde{\chi}_1^0$, respectively. The colour code denotes the size of the respective branching ratio, which is zero below the kinematic thresholds.[9] These rainbow plots show that in case of enhanced photonic rates such non-standard Higgs decays always remain below about 10–20%. The reduced cross section $\mu_{\gamma\gamma}$ is suppressed in case of sizeable branching ratios above ∼0.25 with a maximum of $BR^{\max}_{H_2}(H_1 H_1) \approx 0.36$ and $BR^{\max}_{H_2}(\tilde{\chi}_1^0 \tilde{\chi}_1^0) \approx 0.43$. They are small enough not to be excluded by the present experimental bounds. As can be read off Fig. 7(left), the largest enhancements in the photon final state occur for almost degenerate H_1 and H_2 masses, which corresponds to neutralino masses around 73 GeV, see Fig. 7(right). We explicitly verified that here the enhanced rate in the photon final state is due to the increased branching ratio into photons because of suppressed H_2 couplings to b quarks in this case. Due to sum rules the H_1 coupling to b quarks is then substantial. The combination of the effects of Higgs couplings to SM particles and experimental exclusion limits then implies the observed pattern in the plots. Concerning H_1, it mainly decays into b quark pairs with a branching ratio of 0.8–0.9, followed by decays into τ pairs and a branching ratio of roughly 0.1. The Higgs-to-Higgs or Higgs-to-neutralino decays hence lead to interesting final state signatures with *e.g.* $4b$, $2b2\tau$, 4τ or even multi-μ final states in the former case, from the secondary Higgs decays. In the latter case the final state lightest neutralino entails large missing energy. Such events could act as smoking gun signatures for extended Higgs sectors beyond the minimal SUSY version.

5.3. Compatibility with the LHC Higgs search results

In this subsection we investigate the compatibility of the results for the reduced cross sections μ_{XX} with the experimental best fit values of the signal strengths in the various final states.

[9] Note that we did not consider off-shell decays here.

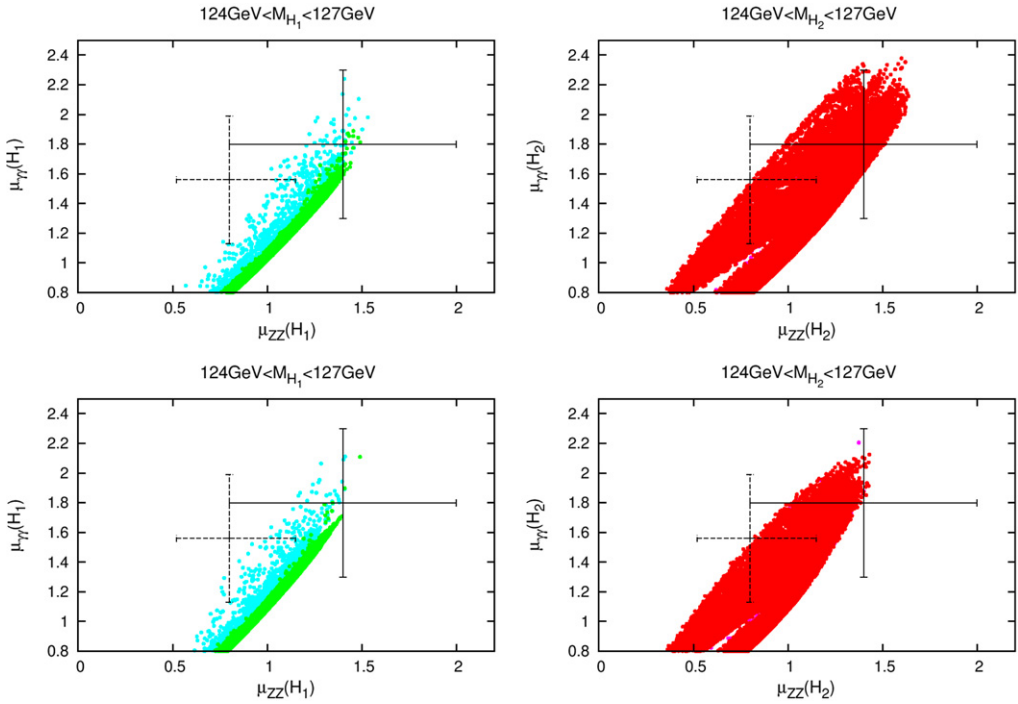

Fig. 8. Reduced cross section into $\gamma\gamma$ versus the reduced cross section into ZZ for $A_t = 0$ GeV (upper) and $A_t = 1$ TeV (lower) with $h = H_1$ (left) and $h = H_2$ (right). Cyan/pink points indicate the signals where at least two Higgs bosons with similar masses overlap and the combined reduced cross section deviates by more than 10% from the reduced cross section of the individual Higgs boson. Bars: Experimentally measured values with error bars (full/ATLAS, dashed/CMS). (For interpretation of the references to colour in this figure legend, the reader is referred to the web version of this article.)

Figs. 8–11 show the reduced cross section in the $\gamma\gamma$ final state compared to the one in ZZ, WW, bb and $\tau\tau$, respectively, for $h = H_1$ and H_2 with $A_t = 0$ GeV and $A_t = 1$ TeV. The bars represent the newest results for the best fit values of the signal strengths $\mu = \sigma/\sigma_{\rm SM}$ in the different final states, reported by the ATLAS [1,65–67] and CMS Collaborations [2,68–71], together with their corresponding errors. The values and errors are listed in Table 1 in Appendix A. First of all the plots demonstrate that both H_1 and H_2 can have a mass around 126 GeV and be compatible with the experiment, for small and for large mixing in the stop sector. Moreover an enhancement in the photon rate by up to a factor $\sim$2.4 is possible. The allowed parameter regions are somewhat more extended for $A_t = 0$ GeV, which is an interplay between the production cross section and decay into photon pairs leading to more important reduced rates for the small mixing case. The regions in cyan (pink) indicate where additional Higgs bosons close in mass join $h = H_1$ ($h = H_2$) to build up the signal and lead to reduced cross sections that differ by more than 10% from the one of h alone. Depending on the value of A_t and the final state these regions are more or less extended: The experimental resolution in the various final states is not the same, which has been taken into account by applying a different width in the Gaussian smearing of the non-h Higgs cross sections, that are added to the h final state. Therefore the parameter regions with several Higgs bosons contributing to the final state are for WW final states, where the Higgs mass cannot be reconstructed, different from the ones for ZZ. The same holds for the fermionic final states.

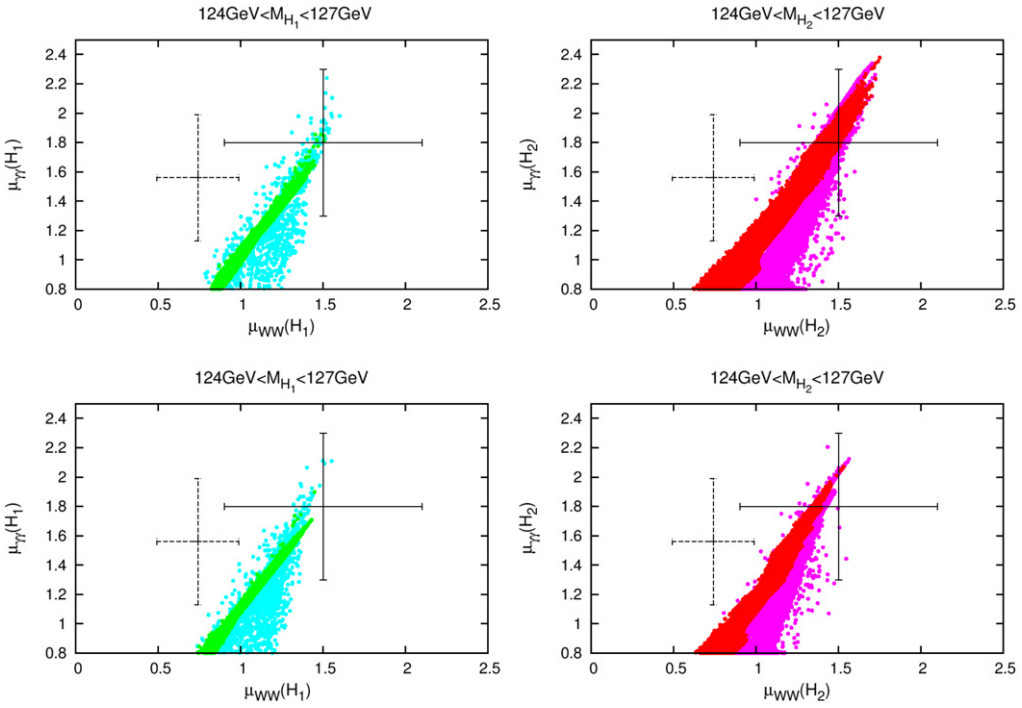

Fig. 9. Reduced cross section into $\gamma\gamma$ versus the reduced cross section into WW for $A_t = 0$ GeV (upper) and $A_t = 1$ TeV (lower) with $h = H_1$ (left) and $h = H_2$ (right). Cyan/pink points indicate the signals where at least two Higgs bosons with similar masses overlap and the combined reduced cross section deviates by more than 10% from the reduced cross section of the individual Higgs boson. Bars: Experimentally measured values with error bars (full/ATLAS, dashed/CMS). (For interpretation of the references to colour in this figure legend, the reader is referred to the web version of this article.)

Here the resolution in the $\tau\tau$ final states is less good than the one in bb, leading to the 'nose' in the plots for $h = H_1$ Fig. 11(left) against the $\tau\tau$ final state.[10] Another reason for the difference in the extensions of the parameter regions is that due to the different Higgs–gauge and Higgs–fermion coupling structures, for a lot of parameter points the non-h Higgs state contributions to the gauge boson final states cannot be important enough to induce a change in the rate by more than 10%. This is because the Higgs–gauge couplings for small values of $\tan\beta$ are dominated by the up-type Higgs component. In order to achieve a large enough production for the h Higgs boson through gluon fusion its up-type component must be near the SM value, inducing a very small up-type component for the other CP-even Higgs bosons due to coupling sum rules, so that they hardly decay into massive gauge bosons. The down-type component of the Higgs bosons, however, has not been restricted and therefore both the h Higgs boson and the other one(s) with mass close to 126 GeV can have equally important couplings to down-type quarks depending on the amount of singlet–doublet mixing.

A substantial amount of scenarios compatible with an excess in the photon final state is hence only due to a superposition of Higgs rates stemming from nearly degenerate Higgs bosons. The

[10] The difference in the bb and $\tau\tau$ branching ratios due to QCD corrections is small enough not to play a significant role here; nor do the negligible Δ_b corrections.

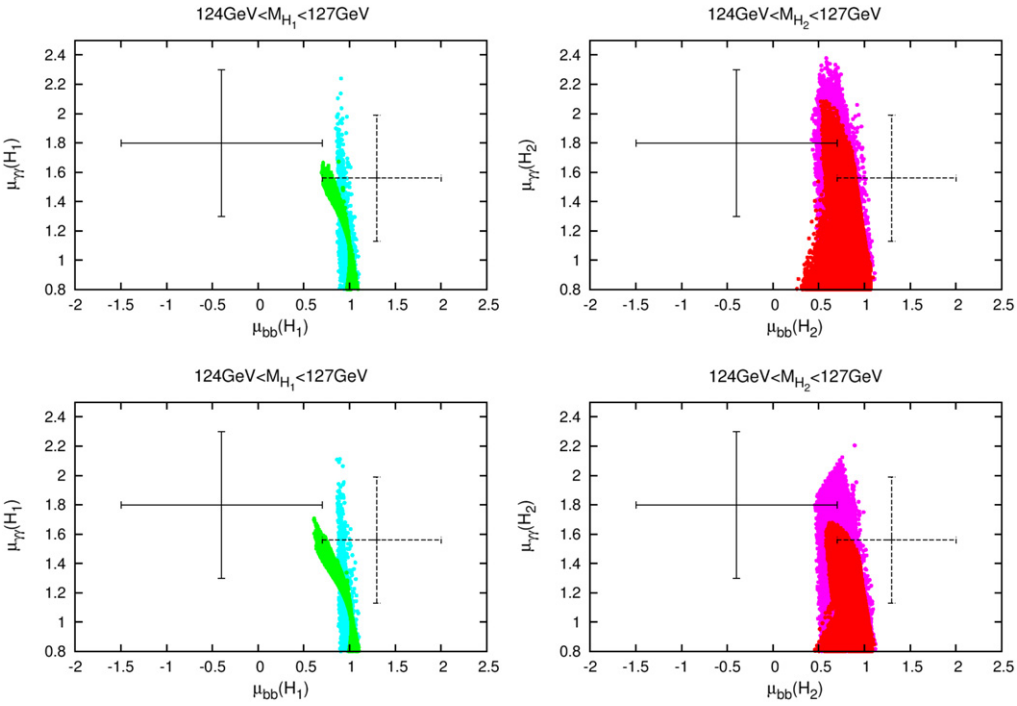

Fig. 10. Reduced cross section into $\gamma\gamma$ versus the reduced cross section into bb for $A_t = 0$ GeV (upper) and $A_t = 1$ TeV (lower) with $h = H_1$ (left) and $h = H_2$ (right). Cyan/pink points indicate the signals where at least two Higgs bosons with similar masses overlap and the combined reduced cross section deviates by more than 10% from the reduced cross section of the individual Higgs boson. Bars: Experimentally measured values with error bars (full/ATLAS, dashed/CMS). (For interpretation of the references to colour in this figure legend, the reader is referred to the web version of this article.)

experimental distinction of such scenarios from single Higgs rates, as has been discussed *e.g.* in Ref. [39], would be a clear signal of beyond the SM Higgs physics.

The plots show the strong correlation between the $\gamma\gamma$ and the massive gauge boson final states: In case the increase in the photonic final state is due to an enhanced photon branching ratio caused by a suppression in the decay width into bb, this affects the branching ratio into gauge bosons as well and leads also here to larger rates. Should the gauge boson reduced cross sections turn out to be exactly SM-like, a strongly enhanced rate into the $\gamma\gamma$ final state would be difficult to comply with. Nevertheless, even in this case enhanced photonic rates up to $\sim$1.6–1.8 are still possible. At the present status of experimental errors and experimental resolution everything is still compatible. There is a little bit more tension with the CMS results, as CMS finds suppressed rates into ZZ, WW contrary to ATLAS reporting enhanced rates. With more data accumulated by the experiments and reduced errors on the μ_{XX} values future will show which of these scenarios will survive and which will be excluded. The correlation between the photon and the fermion final states on the other hand is much less pronounced. While in the gauge boson final states the branching ratios are simultaneously affected by a change in the bb decay mode, the down-type fermion final states are less sensitive to such a change. In the bb final state the μ value reported by ATLAS lies below the allowed regions, the one of CMS above, both still compatible within the large errors with the results of the parameter scan so that at present no conclusive statement

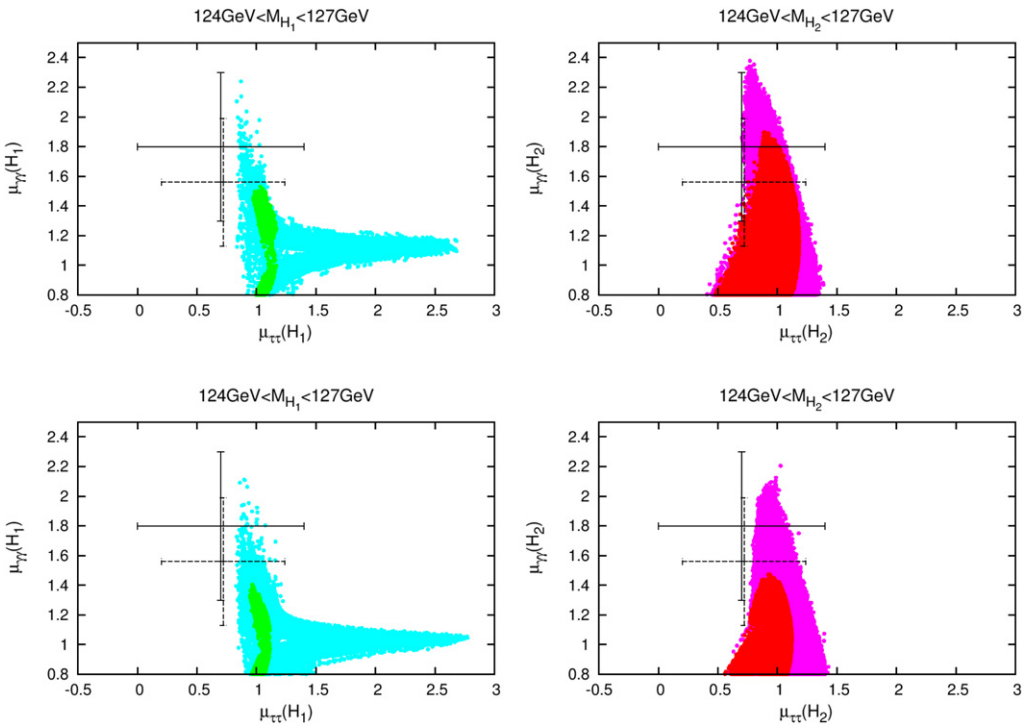

Fig. 11. Reduced cross section into $\gamma\gamma$ versus the reduced cross section into $\tau\tau$ for $A_t = 0$ GeV (upper) and $A_t = 1$ TeV (lower) with $h = H_1$ (left) and $h = H_2$ (right). Cyan/pink points indicate the signals where at least two Higgs bosons with similar masses overlap and the combined reduced cross section deviates by more than 10% from the reduced cross section of the individual Higgs boson. Bars: Experimentally measured values with error bars (full/ATLAS, dashed/CMS). (For interpretation of the references to colour in this figure legend, the reader is referred to the web version of this article.)

can be made. In the $\tau\tau$ final state the reported μ value is below one and hence the Higgs–$\tau\tau$ coupling suppressed. The ATLAS and CMS values are on the left border of the allowed parameter range and compatible within errors, which also in this channel are still too large to make firm statements.

Concerning perturbativity constraints the regions shown in Figs. 8–11 are mostly compatible within the NMSSM without the inclusion of extra matter. A few scenarios require the inclusion of extra matter at 1 TeV. In case of $\tan\beta = 4$ the shapes of the parameter regions corresponding to Figs. 8–11 stay approximately the same but are much less dense in the amount of allowed scenarios.

With increasing data the precision on the signal strengths reported by the experiments will improve and the exclusion limits will become more stringent. This has to be taken into account when combining signals stemming from two Higgs bosons which are close in mass. Thereby the reduced cross sections μ_{XX} will change. In particular the enhancement in the $\gamma\gamma$ final state, which in a substantial amount of scenarios is due to this superposition, may partially disappear. Furthermore, it affects scenarios which have been excluded due to too large signal rates from the combination of two Higgs signals. On the other hand, the improved precision would then reveal two Higgs signals lying close to each other, providing an unambiguous sign of BSM physics, should the NMSSM or some other multi-Higgs sector be realised in nature.

6. Summary and outlook

In this paper we have studied the phenomenology of Higgs bosons close to 126 GeV within the scale invariant unconstrained NMSSM, focusing on the regions of parameter space favoured by low fine-tuning considerations, namely stop masses of order 400 GeV to 1 TeV and an effective μ parameter between 100–200 GeV, with large λ (which is required to remain perturbative up to the GUT scale) and low $\tan\beta = 2$–4.

By performing scans over the above parameter space, focusing on the observable Higgs cross sections into $\gamma\gamma$, WW, ZZ, bb and $\tau\tau$ final states, we have studied the correlations between these observables. Although we examined only a limited parameter range in A_κ, A_λ and κ, we found a substantial amount of parameter space which can lead to Higgs boson masses and couplings compatible with the latest LHC results.

There are basically two types of NMSSM scenarios compatible with the data, corresponding to the 126 GeV Higgs boson being either the lightest CP-even Higgs boson H_1 or the second lightest one H_2. Our results clearly favour the second option, however the first option is still possible but it requires additional extra matter at the TeV scale in order to maintain the perturbativity of λ, as well as large stop mixing and low $\tan\beta \sim 2$ (for example $\tan\beta = 4$ is not allowed) and even then the allowed parameter space is relatively sparse. We emphasise that these conclusions only apply to the natural NMSSM, in the low fine-tuning region defined above, and that larger stop masses and mixing (above one TeV) would allow a larger parameter space with H_1 at 126 GeV.

The enhancement in the Higgs rate in the di-photon channel that we observe in our results is due to a combination of factors. Firstly there can be an enhancement in the dominant gluon fusion Higgs production cross section due to the light squarks in the loop, where light stops are a feature of the low fine-tuning region. Secondly the Higgs branching ratio in the di-photon channel can be enhanced due to two sub-factors, namely (i) an increased di-photon partial width, induced by stop, charged Higgs and chargino loops, and (ii) a suppressed total width, due to a suppressed Higgs coupling to b quarks resulting from singlet–doublet mixing. Concerning case (i), the stop loop effect in the photonic decay is opposite to the one in gluon fusion and depends on the mixing. In the case (ii) also the rates into the fermionic final states can be suppressed. The reported best fit values of the signal strengths μ in the bb and $\tau\tau$ final states by ATLAS and CMS still suffer from large errors, so that it is difficult to draw a conclusion on possibly suppressed couplings to down-type fermions. The allowed parameter ranges we found for enhanced di-photon event rates are compatible with the experimental best fits of the μ values in the various final states.

Although our results encompass the SM case where all μ values are equal to unity, we also allow for significant and correlated departures from unity for all channels. While we do not find any significant correlation between di-photon and fermion rates (μ values), we do find a correlation between the di-photon and massive gauge boson rates (μ values). However, given the present status of the experimental accuracy in the various final states, it is not possible to draw any conclusions about this. Nevertheless it is clear that the natural NMSSM Higgs sector (corresponding to the low fine-tuning region as defined above) is nicely compatible with all experimental results, with the bulk of the data points corresponding to the second lightest Higgs boson H_2 having a mass of about 126 GeV. In this favoured case, the 126 GeV H_2 boson can decay into pairs of lighter neutralinos, CP-even or CP-odd Higgs bosons, providing a smoking gun signature of the NMSSM.

We also emphasise that a good part of the parameter space involves a Higgs spectrum where the two lighter CP-even Higgs bosons H_1 and H_2 are close in mass. It is then the combination

of their reduced cross sections and rates which is observed in the experiment. However, with increasing accuracy in the Higgs boson mass resolution, future LHC data may resolve these two states. Observing the two separate CP-even Higgs bosons H_1 and H_2 with different masses would not only rule out the Standard Model, but could also provide direct evidence for the Higgs sector of the NMSSM.

With future LHC results, the best fit values of the signal strengths and their errors in the different channels will change, leading to different positions and error bars on the data points represented by crosses in our plots. However, the overall pattern of the plots themselves will not change substantially. Thus future data can be compared to our predictions to check the compatibility of the natural NMSSM with experiment. If stops are not discovered below one TeV, and instead the experimental limit on the stop masses increases, then the range of the stop masses and mixing may need to be extended beyond the low fine-tuned region considered here, leading to enlarged parameter regions of the NMSSM. However, for the moment, the natural NMSSM is still viable, with the characteristic Higgs spectrum and properties discussed in this paper.

Acknowledgements

M.M. and K.W. are supported by the DFG SFB/TR9 "Computational Particle Physics". S.F.K. is supported by the STFC Consolidated grant ST/J000396/1 and EU ITN grants UNILHC 237920 and INVISIBLES 289442. We would like to thank Günter Quast and Markus Schumacher for very helpful discussions. M.M. furthermore thanks Wim de Boer for interesting conversations on NMSSM and Dark Matter. R.N. is grateful to M.I. Vysotsky and L.B. Okun for fruitful discussions.

Appendix A. Best fit values of the signal strength

We list the best fit values of the signal strengths $\mu = \sigma/\sigma_{\rm SM}$ in the various final states reported by ATLAS [1,65–67] and CMS [2,68–71], which we have applied in our plots.[11]

Table 1
Best fit values of the signal strength μ in the $\gamma\gamma$, WW, ZZ, bb and $\tau\tau$ final states reported by ATLAS [1,65–67] and CMS [2,68–71].

Experiment	Final state	$(\sqrt{s}, L)$	$\mu = \sigma/\sigma_{\rm SM}$
ATLAS	$\gamma\gamma$	(7 TeV, 4.8 fb^{-1}) + (8 TeV, 5.9 fb^{-1})	1.8 ± 0.5 [1]
	WW	(8 TeV, 13 fb^{-1})	1.5 ± 0.6 [65]
	ZZ	(7 TeV, 4.8 fb^{-1}) + (8 TeV, 5.8 fb^{-1})	1.4 ± 0.6 [1]
	bb	(7 TeV, 4.7 fb^{-1}) + (8 TeV, 13 fb^{-1})	-0.4 ± 1.1[66]
	$\tau\tau$	(7 TeV, 4.6 fb^{-1}) + (8 TeV, 13 fb^{-1})	0.7 ± 0.7 [67]
CMS	$\gamma\gamma$	(7 TeV, 5.1 fb^{-1}) + (8 TeV, 5.3 fb^{-1})	1.56 ± 0.43 [2]
	WW	(7 TeV, 4.9 fb^{-1}) + (8 TeV, 12.1 fb^{-1})	0.74 ± 0.25 [68]
	ZZ	(7 TeV, 5.1 fb^{-1}) + (8 TeV, 12.2 fb^{-1})	$0.8^{+0.35}_{-0.28}$ [69]
	bb	(7 TeV, 5 fb^{-1}) + (8 TeV, 12 fb^{-1})	$1.3^{+0.7}_{-0.6}$ [70]
	$\tau\tau$	(7 TeV + 8 TeV, 17 fb^{-1})	0.72 ± 0.52 [71]

[11] The statistical (± 0.7) and systematic error (± 0.8) in the bb final state reported by ATLAS have been added in quadrature.

References

[1] G. Aad, et al., ATLAS Collaboration, Phys. Lett. B 716 (2012) 1, arXiv:1207.7214 [hep-ex];
G. Aad, et al., ATLAS Collaboration, ATLAS-CONF-2012-162.
[2] S. Chatrchyan, et al., CMS Collaboration, Phys. Lett. B 716 (2012) 30, arXiv:1207.7235 [hep-ex];
S. Chatrchyan, et al., CMS Collaboration, CMS-PAS-HIG-12-045.
[3] C. Englert, T. Plehn, M. Rauch, D. Zerwas, P.M. Zerwas, Phys. Lett. B 707 (2012) 512, arXiv:1112.3007 [hep-ph];
J.R. Espinosa, C. Grojean, M. Muhlleitner, M. Trott, JHEP 1205 (2012) 097, arXiv:1202.3697 [hep-ph];
P.P. Giardino, K. Kannike, M. Raidal, A. Strumia, JHEP 1206 (2012) 117, arXiv:1203.4254 [hep-ph];
J. Ellis, T. You, JHEP 1206 (2012) 140, arXiv:1204.0464 [hep-ph];
A. Azatov, R. Contino, D. Del Re, J. Galloway, M. Grassi, S. Rahatlou, JHEP 1206 (2012) 134, arXiv:1204.4817 [hep-ph];
M. Klute, R. Lafaye, T. Plehn, M. Rauch, D. Zerwas, Phys. Rev. Lett. 109 (2012) 101801, arXiv:1205.2699 [hep-ph];
A. Azatov, R. Contino, J. Galloway, arXiv:1206.3171 [hep-ph];
I. Low, J. Lykken, G. Shaughnessy, arXiv:1207.1093 [hep-ph];
T. Corbett, O.J.P. Eboli, J. Gonzalez-Fraile, M.C. Gonzalez-Garcia, arXiv:1207.1344 [hep-ph];
P.P. Giardino, K. Kannike, M. Raidal, A. Strumia, arXiv:1207.1347 [hep-ph];
J. Ellis, T. You, JHEP 1209 (2012) 123, arXiv:1207.1693 [hep-ph];
J.R. Espinosa, C. Grojean, M. Muhlleitner, M. Trott, arXiv:1207.1717 [hep-ph];
D. Carmi, A. Falkowski, E. Kuflik, T. Volansky, J. Zupan, arXiv:1207.1718 [hep-ph];
F. Bonnet, T. Ota, M. Rauch, W. Winter, arXiv:1207.4599 [hep-ph];
T. Plehn, M. Rauch, Europhys. Lett. 100 (2012) 11002, arXiv:1207.6108 [hep-ph];
G. Moreau, arXiv:1210.3977 [hep-ph].
[4] G.L. Kane, G.D. Kribs, S.P. Martin, J.D. Wells, Phys. Rev. D 53 (1996) 213, hep-ph/9508265;
S. Dawson, A. Djouadi, M. Spira, Phys. Rev. Lett. 77 (1996) 16, hep-ph/9603423;
M. Muhlleitner, M. Spira, Nucl. Phys. B 790 (2008) 1, hep-ph/0612254.
[5] A. Djouadi, Phys. Lett. B 435 (1998) 101, hep-ph/9806315.
[6] M. Carena, S. Gori, N.R. Shah, C.E.M. Wagner, JHEP 1203 (2012) 014, arXiv:1112.3336 [hep-ph];
M. Carena, S. Gori, N.R. Shah, C.E.M. Wagner, L.-T. Wang, JHEP 1207 (2012) 175, arXiv:1205.5842 [hep-ph];
M.A. Ajaib, I. Gogoladze, Q. Shafi, arXiv:1207.7068 [hep-ph].
[7] K. Schmidt-Hoberg, F. Staub, arXiv:1208.1683 [hep-ph].
[8] D. Carmi, A. Falkowski, E. Kuflik, T. Volansky, JHEP 1207 (2012) 136, arXiv:1202.3144 [hep-ph];
N. Desai, B. Mukhopadhyaya, S. Niyogi, arXiv:1202.5190 [hep-ph];
J.R. Espinosa, C. Grojean, V. Sanz, M. Trott, arXiv:1207.7355 [hep-ph];
A. Arbey, M. Battaglia, A. Djouadi, F. Mahmoudi, JHEP 1209 (2012) 107, arXiv:1207.1348 [hep-ph];
M.R. Buckley, D. Hooper, arXiv:1207.1445 [hep-ph];
H. An, T. Liu, L.-T. Wang, arXiv:1207.2473 [hep-ph];
Z. Kang, T. Li, J. Li, Y. Liu, arXiv:1208.2673 [hep-ph];
Z. Heng, arXiv:1210.3751 [hep-ph].
[9] A. Arvanitaki, G. Villadoro, JHEP 1202 (2012) 144, arXiv:1112.4835 [hep-ph].
[10] K. Hagiwara, J.S. Lee, J. Nakamura, JHEP 1210 (2012) 002, arXiv:1207.0802 [hep-ph].
[11] R. Benbrik, M.G. Bock, S. Heinemeyer, O. Stal, G. Weiglein, L. Zeune, Eur. Phys. J. C 72 (2012) 2171, arXiv:1207.1096 [hep-ph].
[12] G. Belanger, U. Ellwanger, J.F. Gunion, Y. Jiang, S. Kraml, arXiv:1208.4952 [hep-ph].
[13] K. Choi, S.H. Im, K.S. Jeong, M. Yamaguchi, arXiv:1211.0875 [hep-ph].
[14] U. Ellwanger, JHEP 1203 (2012) 044, arXiv:1112.3548 [hep-ph].
[15] Z. Kang, J. Li, T. Li, arXiv:1201.5305 [hep-ph];
J. Cao, Z. Heng, J.M. Yang, J. Zhu, JHEP 1210 (2012) 079, arXiv:1207.3698 [hep-ph].
[16] U. Ellwanger, Phys. Lett. B 698 (2011) 293, arXiv:1012.1201 [hep-ph];
J. Cao, Z. Heng, T. Liu, J.M. Yang, Phys. Lett. B 703 (2011) 462, arXiv:1103.0631 [hep-ph].
[17] A. Azatov, S. Chang, N. Craig, J. Galloway, Phys. Rev. D 86 (2012) 075033, arXiv:1206.1058 [hep-ph].
[18] L.J. Hall, D. Pinner, J.T. Ruderman, JHEP 1204 (2012) 131, arXiv:1112.2703 [hep-ph].
[19] S.F. King, M. Muhlleitner, R. Nevzorov, Nucl. Phys. B 860 (2012) 207, arXiv:1201.2671 [hep-ph].
[20] F. Boudjema, G.D. La Rochelle, Phys. Rev. D 86 (2012) 015018, arXiv:1203.3141 [hep-ph];
N.D. Christensen, T. Han, S. Su, Phys. Rev. D 85 (2012) 115018, arXiv:1203.3207 [hep-ph].

[21] J.-J. Cao, Z.-X. Heng, J.M. Yang, Y.-M. Zhang, J.-Y. Zhu, JHEP 1203 (2012) 086, arXiv:1202.5821 [hep-ph].
[22] D.A. Vasquez, G. Belanger, C. Boehm, J. Da Silva, P. Richardson, C. Wymant, Phys. Rev. D 86 (2012) 035023, arXiv:1203.3446 [hep-ph].
[23] U. Ellwanger, C. Hugonie, Adv. High Energy Phys. 2012 (2012) 625389, arXiv:1203.5048 [hep-ph].
[24] G. Belanger, U. Ellwanger, J.F. Gunion, Y. Jiang, S. Kraml, J.H. Schwarz, arXiv:1210.1976 [hep-ph].
[25] A. Djouadi, Phys. Rep. 459 (2008) 1–241, hep-ph/0503173.
[26] B. de Carlos, J.A. Casas, Phys. Lett. B 309 (1993) 320, hep-ph/9303291;
P.H. Chankowski, J.R. Ellis, S. Pokorski, Phys. Lett. B 423 (1998) 327, hep-ph/9712234;
R. Barbieri, A. Strumia, Phys. Lett. B 433 (1998) 63, hep-ph/9801353;
G.L. Kane, S.F. King, Phys. Lett. B 451 (1999) 113, hep-ph/9810374;
L. Giusti, A. Romanino, A. Strumia, Nucl. Phys. B 550 (1999) 3, hep-ph/9811386;
Z. Chacko, Y. Nomura, D. Tucker-Smith, Nucl. Phys. B 725 (2005) 207, hep-ph/0504095;
R. Kitano, Y. Nomura, Phys. Lett. B 631 (2005) 58, hep-ph/0509039;
P. Athron, D.J. Miller, Phys. Rev. D 76 (2007) 075010, arXiv:0705.2241 [hep-ph];
S. Cassel, D.M. Ghilencea, G.G. Ross, Nucl. Phys. B 825 (2010) 203, arXiv:0903.1115 [hep-ph];
R. Barbieri, D. Pappadopulo, JHEP 0910 (2009) 061, arXiv:0906.4546 [hep-ph];
M. Asano, H.D. Kim, R. Kitano, Y. Shimizu, JHEP 1012 (2010) 019, arXiv:1010.0692 [hep-ph].
[27] M. Bastero-Gil, C. Hugonie, S.F. King, D.P. Roy, S. Vempati, Phys. Lett. B 489 (2000) 359, hep-ph/0006198;
A. Delgado, C. Kolda, J.P. Olson, A. de la Puente, Phys. Rev. Lett. 105 (2010) 091802, arXiv:1005.1282 [hep-ph];
U. Ellwanger, G. Espitalier-Noel, C. Hugonie, JHEP 1109 (2011) 105, arXiv:1107.2472 [hep-ph];
G.G. Ross, K. Schmidt-Hoberg, arXiv:1108.1284 [hep-ph].
[28] M. Perelstein, B. Shakya, arXiv:1208.0833 [hep-ph];
K. Agashe, Y. Cui, R. Franceschini, arXiv:1209.2115 [hep-ph].
[29] P. Fayet, Nucl. Phys. B 90 (1975) 104;
P. Fayet, Phys. Lett. B 64 (1976) 159;
P. Fayet, Phys. Lett. B 69 (1977) 489;
P. Fayet, Phys. Lett. B 84 (1979) 416;
H.P. Nilles, M. Srednicki, D. Wyler, Phys. Lett. B 120 (1983) 346;
J.M. Frere, D.R. Jones, S. Raby, Nucl. Phys. B 222 (1983) 11;
J.P. Derendinger, C.A. Savoy, Nucl. Phys. B 237 (1984) 307;
A.I. Veselov, M.I. Vysotsky, K.A. Ter-Martirosian, Sov. Phys. JETP 63 (1986) 489;
J.R. Ellis, J.F. Gunion, H.E. Haber, L. Roszkowski, F. Zwirner, Phys. Rev. D 39 (1989) 844;
M. Drees, Int. J. Mod. Phys. A 4 (1989) 3635.
[30] U. Ellwanger, M. Rausch de Traubenberg, C.A. Savoy, Phys. Lett. B 315 (1993) 331;
U. Ellwanger, M. Rausch de Traubenberg, C.A. Savoy, Z. Phys. C 67 (1995) 665;
U. Ellwanger, M. Rausch de Traubenberg, C.A. Savoy, Nucl. Phys. B 492 (1997) 307;
U. Ellwanger, Phys. Lett. B 303 (1993) 271;
P. Pandita, Z. Phys. C 59 (1993) 575;
T. Elliott, S.F. King, P.L. White, Phys. Rev. D 49 (1994) 2435;
S.F. King, P.L. White, Phys. Rev. D 52 (1995) 4183;
F. Franke, H. Fraas, Int. J. Mod. Phys. A 12 (1997) 479.
[31] S.F. King, P.L. White, Phys. Rev. D 53 (1996) 4049, hep-ph/9508346;
G.G. Ross, K. Schmidt-Hoberg, F. Staub, JHEP 1208 (2012) 074, arXiv:1205.1509 [hep-ph];
G.G. Ross, K. Schmidt-Hoberg, Nucl. Phys. B 862 (2012) 710, arXiv:1108.1284 [hep-ph];
C. Balazs, M.S. Carena, A. Freitas, C.E.M. Wagner, JHEP 0706 (2007) 066, arXiv:0705.0431 [hep-ph];
C. Panagiotakopoulos, K. Tamvakis, Phys. Lett. B 446 (1999) 224;
C. Panagiotakopoulos, K. Tamvakis, Phys. Lett. B 469 (1999) 145;
C. Panagiotakopoulos, A. Pilaftsis, Phys. Rev. D 63 (2001) 055003;
A. Dedes, C. Hugonie, S. Moretti, K. Tamvakis, Phys. Rev. D 63 (2001) 055009;
A. Menon, D.E. Morrissey, C.E.M. Wagner, Phys. Rev. D 70 (2004) 035005;
T. Han, P. Langacker, B. McElrath, Phys. Rev. D 70 (2004) 115006.
[32] D.J. Miller, R. Nevzorov, P.M. Zerwas, Nucl. Phys. B 681 (2004) 3, hep-ph/0304049.
[33] U. Ellwanger, C. Hugonie, A.M. Teixeira, Phys. Rep. 496 (2010) 1, arXiv:0910.1785 [hep-ph];
U. Ellwanger, Eur. Phys. J. C 71 (2011) 1782, arXiv:1108.0157 [hep-ph].
[34] M. Maniatis, Int. J. Mod. Phys. A 25 (2010) 3505, arXiv:0906.0777 [hep-ph].
[35] M. Masip, R. Munoz-Tapia, A. Pomarol, Phys. Rev. D 57 (1998) R5340, hep-ph/9801437.

[36] J.P. Hall, S.F. King, arXiv:1209.4657 [hep-ph].
[37] J.F. Gunion, Y. Jiang, S. Kraml, Phys. Lett. B 710 (2012) 454, arXiv:1201.0982 [hep-ph];
K. Kowalska, S. Munir, L. Roszkowski, E.M. Sessolo, S. Trojanowski, Y.-L.S. Tsai, arXiv:1211.1693 [hep-ph].
[38] T. Graf, R. Grober, M. Muhlleitner, H. Rzehak, K. Walz, JHEP 1210 (2012) 122, arXiv:1206.6806 [hep-ph].
[39] J.F. Gunion, Y. Jiang, S. Kraml, arXiv:1207.1545 [hep-ph];
J.F. Gunion, Y. Jiang, S. Kraml, arXiv:1208.1817 [hep-ph].
[40] B. Kyae, J.-C. Park, arXiv:1207.3126 [hep-ph].
[41] K.J. Bae, K. Choi, E.J. Chun, S.H. Im, C.B. Park, C.S. Shin, arXiv:1208.2555 [hep-ph].
[42] I. Gogoladze, B. He, Q. Shafi, arXiv:1209.5984 [hep-ph].
[43] K. Schmidt-Hoberg, F. Staub, M.W. Winkler, arXiv:1211.2835 [hep-ph].
[44] K. Kowalska, S. Munir, L. Roszkowski, E.M. Sessolo, S. Trojanowski, Y.-L.S. Tsai, arXiv:1211.1693 [hep-ph].
[45] M. Cvetic, D.A. Demir, J.R. Espinosa, L.L. Everett, P. Langacker, Phys. Rev. D 56 (1997) 2861;
M. Cvetic, D.A. Demir, J.R. Espinosa, L.L. Everett, P. Langacker, Phys. Rev. D 58 (1998) 119905 (Erratum);
P. Langacker, J. Wang, Phys. Rev. D 58 (1998) 115010;
C. Panagiotakopoulos, K. Tamvakis, Phys. Lett. B 446 (1999) 224;
C. Panagiotakopoulos, K. Tamvakis, Phys. Lett. B 469 (1999) 145;
C. Panagiotakopoulos, A. Pilaftsis, Phys. Rev. D 63 (2001) 055003;
A. Dedes, C. Hugonie, S. Moretti, K. Tamvakis, Phys. Rev. D 63 (2001) 055009;
A. Menon, D.E. Morrissey, C.E.M. Wagner, Phys. Rev. D 70 (2004) 035005;
T. Han, P. Langacker, B. McElrath, Phys. Rev. D 70 (2004) 115006;
G.G. Ross, K. Schmidt-Hoberg, arXiv:1108.1284 [hep-ph];
D.A. Demir, G.L. Kane, T.T. Wang, Phys. Rev. D 72 (2005) 015012;
S.F. King, S. Moretti, R. Nevzorov, Phys. Lett. B 634 (2006) 278;
S.F. King, S. Moretti, R. Nevzorov, Phys. Rev. D 73 (2006) 035009;
V. Barger, P. Langacker, H.S. Lee, G. Shaughnessy, Phys. Rev. D 73 (2006) 115010;
S.F. King, R. Luo, D.J. Miller, R. Nevzorov, JHEP 0812 (2008) 042.
[46] M. Matsuda, M. Tanimoto, Phys. Rev. D 52 (1995) 3100;
N. Haba, Prog. Theor. Phys. 97 (1997) 301;
T. Ibrahim, P. Nath, Phys. Rev. D 58 (1998) 111301, hep-ph/9807501;
T. Ibrahim, P. Nath, Phys. Rev. D 60 (1999) 099902 (Erratum);
K. Funakubo, S. Tao, Prog. Theor. Phys. 113 (2005) 821, hep-ph/0409294;
J.R. Ellis, J.S. Lee, A. Pilaftsis, JHEP 0810 (2008) 049, arXiv:0808.1819 [hep-ph];
M. Boz, Mod. Phys. Lett. A 21 (2006) 243;
K. Cheung, T.-J. Hou, J.S. Lee, E. Senaha, Phys. Rev. D 84 (2011) 015002, arXiv:1102.5679 [hep-ph].
[47] S.W. Ham, J. Kim, S.K. Oh, D. Son, Phys. Rev. D 64 (2001) 035007, hep-ph/0104144;
S.W. Ham, S.K. Oh, D. Son, Phys. Rev. D 65 (2002) 075004;
S.W. Ham, Y.S. Jeong, S.K. Oh, hep-ph/0308264;
K. Funakubo, S. Tao, Prog. Theor. Phys. 113 (2005) 821, hep-ph/0409294;
S.W. Ham, S.H. Kim, S.K. Oh, D. Son, Phys. Rev. D 76 (2007) 115013, arXiv:0708.2755 [hep-ph];
K. Cheung, T.-J. Hou, J.S. Lee, E. Senaha, Phys. Rev. D 82 (2010) 075007, arXiv:1006.1458 [hep-ph].
[48] R.D. Peccei, H.R. Quinn, Phys. Rev. Lett. 38 (1977) 1440;
R.D. Peccei, H.R. Quinn, Phys. Rev. D 16 (1977) 1791.
[49] U. Ellwanger, J.F. Gunion, C. Hugonie, JHEP 0502 (2005) 066;
U. Ellwanger, C. Hugonie, Comput. Phys. Commun. 175 (2006) 290.
[50] U. Ellwanger, C. Hugonie, Comput. Phys. Commun. 177 (2007) 399;
http://www.th.u-psud.fr/NMHDECAY/nmssmtools.html;
See also G. Chalons, F. Domingo, arXiv:1209.6235 [hep-ph].
[51] U. Ellwanger, Phys. Lett. B 303 (1993) 271, hep-ph/9302224;
T. Elliott, S.F. King, P.L. White, Phys. Lett. B 305 (1993) 71, hep-ph/9302202;
T. Elliott, S.F. King, P.L. White, Phys. Lett. B 314 (1993) 56, hep-ph/9305282;
T. Elliott, S.F. King, P.L. White, Phys. Rev. D 49 (1994) 2435, hep-ph/9308309;
P.N. Pandita, Z. Phys. C 59 (1993) 575;
P.N. Pandita, Phys. Lett. B 318 (1993) 338;
U. Ellwanger, C. Hugonie, Phys. Lett. B 623 (2005) 93, hep-ph/0504269;
G. Degrassi, P. Slavich, Nucl. Phys. B 825 (2010) 119, arXiv:0907.4682 [hep-ph];
F. Staub, W. Porod, B. Herrmann, JHEP 1010 (2010) 040, arXiv:1007.4049 [hep-ph];

K. Ender, T. Graf, M. Muhlleitner, H. Rzehak, Phys. Rev. D 85 (2012) 075024, arXiv:1111.4952 [hep-ph].
[52] A. Djouadi, M. Spira, P.M. Zerwas, Phys. Lett. B 264 (1991) 440;
A. Djouadi, M. Spira, P.M. Zerwas, Z. Phys. C 70 (1996) 427;
M. Spira, et al., Nucl. Phys. B 453 (1995) 17;
A. Djouadi, J. Kalinowski, M. Spira, Comput. Phys. Commun. 108 (1998) 56.
[53] A. Djouadi, M.M. Muhlleitner, M. Spira, Acta Phys. Polon. B 38 (2007) 635, hep-ph/0609292.
[54] D. Das, U. Ellwanger, A.M. Teixeira, arXiv:1106.5633 [hep-ph].
[55] M. Muhlleitner, A. Djouadi, Y. Mambrini, Comput. Phys. Commun. 168 (2005) 46, hep-ph/0311167;
M. Muhlleitner, Acta Phys. Polon. B 35 (2004) 2753, hep-ph/0409200.
[56] P.Z. Skands, et al., JHEP 0407 (2004) 036, hep-ph/0311123;
B.C. Allanach, et al., Comput. Phys. Commun. 180 (2009) 8, arXiv:0801.0045 [hep-ph].
[57] G. Belanger, F. Boudjema, A. Pukhov, A. Semenov, Comput. Phys. Commun. 149 (2002) 103, hep-ph/0112278;
G. Belanger, F. Boudjema, A. Pukhov, A. Semenov, Comput. Phys. Commun. 174 (2006) 577, hep-ph/0405253;
G. Belanger, F. Boudjema, A. Pukhov, A. Semenov, Comput. Phys. Commun. 180 (2009) 747, arXiv:0803.2360 [hep-ph];
G. Belanger, et al., Comput. Phys. Commun. 182 (2011) 842, arXiv:1004.1092 [hep-ph].
[58] G. Aad, et al., ATLAS Collaboration, arXiv:1208.1447 [hep-ex];
G. Aad, et al., ATLAS Collaboration, arXiv:1208.2590 [hep-ex];
G. Aad, et al., ATLAS Collaboration, arXiv:1208.4305 [hep-ex];
G. Aad, et al., ATLAS Collaboration, arXiv:1209.2102 [hep-ex];
G. Aad, et al., ATLAS Collaboration, arXiv:1209.4186 [hep-ex];
S. Chatrchyan, et al., CMS Collaboration, JHEP 1208 (2012) 110, arXiv:1205.3933 [hep-ex];
S. Chatrchyan, et al., CMS-PAS-SUS-12-017.
[59] K.-i. Hikasa, M. Kobayashi, Phys. Rev. D 36 (1987) 724;
M. Muhlleitner, E. Popenda, JHEP 1104 (2011) 095, arXiv:1102.5712 [hep-ph].
[60] V.M. Abazov, et al., D0 Collaboration, Phys. Lett. B 665 (2008) 1, arXiv:0803.2263 [hep-ex];
T. Aaltonen, et al., CDF Collaboration, arXiv:1203.4171 [hep-ex].
[61] For a summary of the recent limits on SUSY particle masses see G. Aad, et al., ATLAS Collaboration, ATLAS-CONF-2012-104;
G. Aad, et al., ATLAS Collaboration, ATLAS-CONF-2012-109;
See also https://twiki.cern.ch/twiki/pub/AtlasPublic/CombinedSummaryPlots/AtlasSearches_susy_susy12.pdf;
S. Chatrchyan, et al., CMS Collaboration, CMS-PAS-SUS-11-016;
See also https://twiki.cern.ch/twiki/pub/CMSPublic/SUSYSMSSummaryPlots/dibars.pdf.
[62] G. Aad, et al., ATLAS Collaboration, ATLAS-CONF-2012-075.
[63] G. Aad, et al., ATLAS Collaboration, ATLAS-CONF-2012-091;
G. Aad, et al., ATLAS Collaboration, ATLAS-CONF-2012-092.
[64] S. Chatrchyan, et al., CMS Collaboration, CMS-HIG-12-015.
[65] G. Aad, et al., ATLAS Collaboration, ATLAS-CONF-2012-158.
[66] G. Aad, et al., ATLAS Collaboration, ATLAS-CONF-2012-161.
[67] G. Aad, et al., ATLAS Collaboration, ATLAS-CONF-2012-160.
[68] S. Chatrchyan, et al., CMS Collaboration, CMS-PAS-HIG-12-042.
[69] S. Chatrchyan, et al., CMS Collaboration, CMS-PAS-HIG-12-041.
[70] S. Chatrchyan, et al., CMS Collaboration, CMS-PAS-HIG-12-044.
[71] S. Chatrchyan, et al., CMS Collaboration, CMS-PAS-HIG-12-043.
[72] M. Spira, Fortsch. Phys. 46 (1998) 203, hep-ph/9705337.
[73] D. Graudenz, M. Spira, P.M. Zerwas, Phys. Rev. Lett. 70 (1993) 1372;
M. Spira, A. Djouadi, D. Graudenz, P.M. Zerwas, Phys. Lett. B 318 (1993) 347.
[74] M. Spira, A. Djouadi, D. Graudenz, P.M. Zerwas, Nucl. Phys. B 453 (1995) 17, hep-ph/9504378.
[75] A. Djouadi, Phys. Rep. 459 (2008) 1, hep-ph/0503173.
[76] H.E. Haber, G.L. Kane, Phys. Rep. 117 (1985) 75;
J. Gunion, H. Haber, G. Kane, S. Dawson, The Higgs Hunter's Guide, Addison–Wesley, Reading, MA, 1990.
[77] For an overview of possible final states and for further references see U. Ellwanger, Eur. Phys. J. C 71 (2011) 1782, arXiv:1108.0157 [hep-ph].